Activation of αvβ3 Integrin Alters Fibronectin Fibril Formation in Human Trabecular Meshwork Cells in a ROCK-Independent Manner

Mark S. Filla,[1] Jennifer A. Faralli,[1] Harini Desikan,[1] Jennifer L. Peotter,[1] Abigail C. Wannow,[1] and Donna M. Peters[1,2]

[1]Departments of Pathology & Laboratory Medicine, University of Wisconsin-Madison, Madison, Wisconsin, United States
[2]Department of Ophthalmology and Visual Sciences, University of Wisconsin-Madison, Madison, Wisconsin, United States

Correspondence: Donna M. Peters, Department of Pathology, University of Wisconsin-Medical School, 1300 University Avenue, Madison, WI 53706, USA; dmpeter2@wisc.edu.

Submitted: March 26, 2019
Accepted: August 15, 2019

Citation: Filla MS, Faralli JA, Desikan H, Peotter JL, Wannow AC, Peters DM. Activation of αvβ3 integrin alters fibronectin fibril formation in human trabecular meshwork cells in a ROCK-independent manner. *Invest Ophthalmol Vis Sci*. 2019;60:3897–3913. https://doi.org/10.1167/iovs.19-27171

Purpose. Fibronectin fibrillogenesis is an integrin-mediated process that may contribute to the pathogenesis of primary open-angle glaucoma (POAG). Here, we examined the effects of αvβ3 integrins on fibrillogenesis in immortalized TM-1 cells and human trabecular meshwork (HTM) cells.

Methods. TM-1 cells overexpressing wild-type β3 (WTβ3) or constitutively active β3 (CAβ3) integrin subunits were generated. Control cells were transduced with an empty vector (EV). Deoxycholic acid (DOC) extraction of monolayers, immunofluorescence microscopy, and On-cell western analyses were used to determine levels of fibronectin fibrillogenesis and fibronectin fibril composition (EDA+ and EDB+ fibronectins) and conformation. αvβ3 and α5β1 Integrin levels were determined using fluorescence-activated cell sorting (FACS). Cilengitide and an adenovirus vector expressing WTβ3 or CAβ3 integrin subunits were used to examine the role of αvβ3 integrin in HTM cells. The role of the canonical α5β1 integrin–mediated pathway in fibrillogenesis was determined using the fibronectin-binding peptide FUD, the β1 integrin function-blocking antibody 13, and the Rho kinase (ROCK) inhibitor Y27632.

Results. Activation of αvβ3 integrin enhanced the assembly of fibronectin into DOC-insoluble fibrils in both TM-1 and HTM cells. The formation of fibronectin fibrils was dependent on α5β1 integrin and could be inhibited by FUD. However, fibrillogenesis was unaffected by Y27632. Fibrils assembled by CAβ3 cells also contained high levels of EDA+ and EDB+ fibronectin and fibronectin that was stretched.

Conclusions. αvβ3 Integrin signaling altered the deposition and structure of fibronectin fibrils using a β1 integrin/ROCK-independent mechanism. Thus, αvβ3 integrins could play a significant role in altering the function of fibronectin matrices in POAG.

Keywords: fibronectin, trabecular meshwork, glaucoma, integrins

Primary open-angle glaucoma (POAG) is the most common type of glaucoma in the United States, and a major risk factor for POAG is an elevation in intraocular pressure (IOP).[1–3] There is increasing evidence that higher than normal resistance to aqueous humor outflow from the trabecular meshwork (TM) is responsible for this elevation in IOP.[2,4] Recent studies suggest that excess deposition of extracellular matrix (ECM) proteins, especially fibronectin, could be a key factor in the development of restricted aqueous humor outflow from the anterior segment.[5,6] In addition, both POAG and steroid-induced glaucoma (SIG) are associated with an increased accumulation of various ECM proteins,[7,8] including fibronectin.[9]

This excess deposition of fibronectin has been attributed to elevated levels of TGFβ2 in aqueous humor or in response to treatment with glucocorticoids such as dexamethasone.[10–14] Recent studies suggest that the glucocorticoid- and TGFβ2-induced increases in fibronectin may be related since higher levels of TGFβ2 follow glucocorticoid treatments.[15] TGFβ1- and TGFβ2-induced increases in IOP in a rat model have also been shown to correlate with increased fibronectin labeling within the TM.[16,17]

Fibronectin fibrils are a major component of the ECM in the TM,[18–20] and recent in vitro studies have shown that TM cells produce both the EDA+ and EDB+ fibronectin isoforms.[11,12] Fibronectin is one of the earliest ECM fibrils to be assembled in vivo,[21] and it has been found to act as a scaffold upon which other ECM protein matrices can be assembled.[22–26] Within the TM it appears to be involved in the assembly of nascent matrices of type IV collagen, laminin, and fibrillin into the ECM.[12] Fibronectin fibrils also act as bioreserviors for growth factors such as TGFβ2 and enzymes like LOX1,[26,27] both of which have been implicated in glaucoma.[10,28] The EDA domain of fibronectin has been implicated in the formation of myofibroblasts and fibrosis[29] and is a factor that may play a role in POAG and SIG.[11] Fibronectin fibrils therefore would be expected to play a critical role in maintaining ECM homeostasis in the normal TM and in the development of POAG and SIG.

Unlike some ECM proteins such as type I collagen, the incorporation of fibronectin into fibrils is a multistep process

that involves integrin signaling and the contractile properties of the tissue.[20,30–33] Fibronectin fibril formation is initiated when the secreted soluble protein dimer binds to cell surface integrins. Once bound, the fibronectin dimer is unfolded and stretched, resulting in a conformational change that exposes specific fibronectin–fibronectin binding sites within the molecule that promote the assembly of a larger, insoluble fibril. The unfolding and stretching of the soluble fibronectin dimers is believed to be mediated by the guanosine triphosphatase (GTPase) RhoA and the contractile properties of the actomyosin network.[34]

Integrins are a family of cell surface receptors consisting of a noncovalently bound heterodimer of α and β subunits. At least six fibronectin binding integrins have been identified in the TM,[31] including α5β1, which is the major integrin that mediates fibronectin fibril assembly.[35,36] Several other integrins, however, are capable of initiating fibril assembly including αvβ3 integrin. Expression of the α5, αv, and β3 integrin subunits in TM cells is affected by glucocorticoids,[37] and studies from our lab have shown that the overall levels and activity of αvβ3 integrin in human TM (HTM) cells are increased in response to glucocorticoids such as dexamethasone.[38–41] Although α5β1 and αvβ3 integrin expression is affected by TGFβ1 in other cell types,[42–44] to date only one study has reported that TM cells increased expression of αv and β3 integrin subunits in response to TGFβ2.[45]

Given the important role that fibronectin appears to play in regulating the assembly of the ECM within the TM,[12] we sought to examine the relationship between αvβ3 integrin signaling and fibronectin matrix assembly using an immortalized TM cell line, TM-1, previously engineered to stably overexpress either a wild-type (WTβ3) or constitutively active (CAβ3) αvβ3 integrin,[40] and HTM cells expressing an activated αvβ3 integrin. We specifically looked to see if the activated conformation of αvβ3 integrin was involved. Our previous studies have suggested that this conformation caused HTM cells to exhibit phenotypes associated with POAG and SIG,[40,41,46,47] including actin cytoskeletal rearrangements into cross-linked actin networks (CLANs) and inhibition of phagocytosis. We report here that this activated conformation of αvβ3 integrin also increases fibronectin fibril assembly in TM cells. This increase in fibrils includes multiple fibronectin isoforms, a stretched conformation of fibronectin, and appears to be independent of Rho kinase (ROCK) activity.

Materials and Methods

Materials

Rabbit polyclonal fibronectin antiserum was produced in our lab and validated by ELISA analysis[48] and immunofluorescence microscopy.[12] Normal rabbit serum was purchased from Vector Laboratories (cat. #S-5000; Burlingame, CA, USA). The mouse anti-EDA+ fibronectin clone IST-9 (cat. #ab6328), mouse anti-EDB+ fibronectin clone BC-1 (cat. #ab154210), mouse anti-β3 integrin clone CRC54 (#ab34409), mouse anti-α5 integrin clone P1D6 (cat. #71684), mouse anti-β1 integrin clone 12G10 (cat. #ab30394), and rabbit polyclonal anti-β actin (cat. #ab8227) were purchased from Abcam (Cambridge, MA, USA). A mouse anti-fibronectin clone L8[49] was obtained from Deane Mosher (University of Wisconsin-Madison). Mouse anti-β-galactosidase clone GAL-13 (cat. #G8021) was purchased from Sigma-Aldrich Corp. (St. Louis, MO, USA). The mouse anti-αvβ3 clone LM609 (cat. #MAB1976) and mouse anti-α5 integrin clone SNAKA51 (cat. #MABT201) were purchased from EMD Millipore (Burlington, MA, USA). Rat anti-β1 integrin (CD29) clone 13 (cat. #552828) and rat IgG (cat. #555841) were purchased from BD Biosciences (San Jose, CA, USA). Alexa Fluor 488-phalloidin was purchased from Thermo Fisher Scientific (cat. #A12379; Waltham, MA, USA). The αvβ3-inhibitory peptide cilengitide (cat. #5870) was purchased from Tocris Biosciences (Bristol, UK). The ROCK inhibitor Y27632 (cat. #688000) was purchased from EMD Millipore. Recombinant FUD (functional upstream domain) peptide, derived from the *Streptococcus pyogenes* F1 adhesin protein, was expressed and prepared as previously described.[12]

Adenovirus 5 (Ad5) WTβ3-mCherry/CAβ3-mCherry Construction

The wild-type cDNA for the human β3 integrin subunit was obtained from Thermo Fisher Scientific and cloned into the pLVX-IRES-Puro vector (Takara Bio USA, Mountain View, CA, USA) as previously described.[40] A DNA fragment containing a Kozak sequence was then cloned onto the amino terminus of the β3 integrin cDNA along with an mCherry tag at the carboxyl terminus. This WTβ3 integrin-mCherry transgene was then cloned into the Xho1/Xba1 site of the pacAd5CMVmcsSV40pA shuttle vector (Ad5-WTβ3). Site-directed mutagenesis was used to create the pacAd5CMV-β3 integrin T562N-mCherry-SV40pA vector (Ad5-CAβ3). Cloning and site-directed mutagenesis of the Ad5-WTβ3-mCherry and Ad5-CAβ3-mCherry vectors were done by GenScript (Piscataway, NJ, USA) and validated by cDNA sequencing. The engineered vectors, along with the pacAd5CMVmcsSV40pAAd5 empty vector (Ad5-EV), were each packaged at the University of Iowa Viral Vector Core.

Cell Culture

Immortalized TM-1 cells overexpressing either a wild-type β3 integrin subunit (WTβ3) or a constitutively active $\beta3^{T562N}$ integrin subunit (CAβ3)[50] were generated as previously described.[40] A cell line transfected with an empty vector (EV) was used as a control. All TM-1–derived cell lines were cultured in routine growth medium consisting of low-glucose Dulbecco's modified Eagle's medium (DMEM) (Sigma Aldrich Corp.), 10% fetal bovine serum (FBS) (Atlanta Biologicals, Atlanta, GA, USA), 2 mM L-glutamine (Sigma Aldrich Corp.), 0.2% Primocin (InvivoGen, San Diego, CA, USA), and 0.05% gentamicin (Mediatech, Manassas, VA, USA). Cells were kept under selection in 2 μg/mL puromycin. The N27TM-6 strain of normal HTM cells was isolated from a 27-year-old female donor and characterized as previously described.[51–53] HTM cells were routinely grown in the same growth medium used for TM-1 cell lines except for the use of 15% FBS and 1 ng/mL FGF-2 (PeproTech, Rocky Hill, NJ, USA).

In experiments in which HTM cells were treated with or without cilengitide (CGT) or dexamethasone (DEX) to activate the αvβ3 integrin,[38,41,54] HTM cells were plated at a density of 3×10^4 cells/well in growth medium into 96-well plates. Upon reaching confluence, cells were fed daily with growth medium for 7 days. Cells were then switched to low serum (1% FBS) and treated for 12 to 14 days with control medium, medium plus 0.1% ethanol (vehicle), or 500 nM DEX or medium containing 50, 100, or 200 μM CGT plus either vehicle or DEX. At the end of the treatment period cells were processed for On-cell western (OCW) analysis as described below.

For experiments in which HTM cells were transduced with Ad5 viral vectors expressing mCherry-β3 integrin transgenes, cells were plated at 4×10^4 cells/well in normal growth medium in 24-well plates. Just prior to reaching confluence, cells were transduced with either Ad5-EV, Ad5-WTβ3 integrin-mCherry, or Ad5-$\beta3^{T562N}$ integrin-mCherry for 24 hours at a multiplicity of infection (MOI) of 100. Twenty-four hours post

transduction, cells were refed with normal growth medium. Upon reaching confluence, cells were refed daily with normal growth medium for 7 days. Cells were then refed with 10% FBS-containing medium for 48 hours followed by 1% FBS-containing medium for another 48 hours prior to processing for OCW analysis as described below or immunofluorescence microscopy.

Fluorescence-Activated Cell Sorting (FACS) Analysis

Cells in growth medium were detached from plates using Cell Dissociation Buffer (Sigma Aldrich Corp.) and blocked in PBS plus 5% BSA on ice. They were then incubated with IgG only, mAb LM609, mAb PID6, or mAb 12G10 at 5 μg/mL for 1 hour on ice. Cells were washed and labeled with Alexa Fluor 488 goat anti-mouse IgG (cat. #A11029; Thermo Fisher Scientific) diluted 1:4000 for 30 minutes on ice. The cells were then fixed with PBS + 1% paraformaldehyde (PFA). Data were collected using either a FACSCalibur (Becton Dickinson, Franklin Lakes, NJ, USA) or an Attune NxT (Thermo Fisher Scientific) flow cytometer and analyzed using FlowJo software (FlowJo, LLC, Ashland, OR, USA). The FlowJo software was used to calculate the normal geometric mean fluorescence (NGMF).

On-Cell Western Analysis (OCW)

TM-1–derived cell lines were plated at a density of 5×10^4 cells/well in low-serum (1% FBS) medium into 96-well plates for 3 to 4 hours to allow the cells to attach and spread. The cells were then treated with or without 500 nM FUD, 10 μg/mL mAb 13 or control rat IgG, or 5 μM Y27632 for 24 hours. To determine the level of deoxycholic acid (DOC)-insoluble fibronectin fibrils, cell layers were extracted with 1% DOC-containing buffer and processed for OCW analysis as previously described.[12] To determine the level of fibronectin in either the unextracted or DOC-extracted wells, cell layers or DOC-extracted matrices in the wells were fixed with 4% PFA and labeled with anti-fibronectin antibodies followed by an IRDye 800CW-conjugated secondary antibody. The fibronectin-labeled wells were blanked against wells labeled with normal rabbit serum or an irrelevant mouse mAb. The level of fibronectin labeling was normalized to the total protein content/well as determined by labeling with IRDye 680RD NHS ester. Quantification of the signals at each wavelength was performed using LI-COR Image Studio v. 5.0.21 software (Li-Cor Biosciences, Lincoln, NE, USA). Except where noted in the legend, the results represent the mean ± SE of data pooled from two to six experiments depending upon the exact assay.

MTT Cell Viability Assay

Cells were plated into 96-well plates and allowed to attach for 3 to 4 hours. Cells were refed with media containing 1% FBS with or without 500 nM or 2 μM FUD for 24 hours. As a control, some cells were treated for 24 hours with 0.1% saponin. Viability was determined using a CellQuanti-MTT assay kit (BioAssay Systems, Hayward, CA, USA) as previously described.[12] The results represent the mean ± SE of data pooled from three experiments.

Immunofluorescence Microscopy

Cells were fixed with 4% PFA in PBS at room temperature for 20 minutes and blocked in PBS plus 1% BSA prior to labeling with the various primary antibodies. For immunolabeling studies, cells were labeled with primary antibodies diluted in block. Primary antibodies were detected with Alexa Fluor 488 goat anti-rabbit IgG (cat. #A11034), Alexa Fluor 546 goat anti-mouse IgG (cat. #A11030), Alexa Fluor 546 goat anti-rabbit IgG (cat. #A11035), or Alexa Fluor 488 goat anti-mouse IgG. All secondary antibodies were diluted in block. Alexa Fluor secondary antibodies were purchased from Thermo Fisher Scientific. Nuclei were labeled using Hoechst 33342 (cat. #H1399, Thermo Fisher Scientific). Fluorescence was observed with a Zeiss Imager.Z2 epifluorescence microscope (Carl Zeiss AG, Oberkochen, Germany) equipped with a digital camera (Axiocam 702 mono) and image acquisition software (Zen v. 2.3). All experiments were independently performed two to four times. For the experiments in which cells were treated with or without the ROCK inhibitor Y27632, Z-stacks were acquired from three fields of view/coverslip. Using the image acquisition software, these Z-stacks were then deconvoluted and reconstructed into three-dimensional images or compressed into single images. Cells transduced with Ad5-viral vectors were not labeled with primary or secondary antibodies prior to observation using fluorescence microscopy.

Table. Primers Used for Real-Time RT-PCR

Type	Sequence
Human fibronectin	Forward: CAGGATCACTTACGGAGAAACAG
	Reverse: GCCAGTGACAGCATACACAGTG
Human EDA-fibronectin	Forward: AGGACTGGCATTCACTGATGTG
	Reverse: GTCACCCTGTACCTGGAAACTTG
Human EDB-fibronectin	Forward: CGTGGACCCCGCTAAACTC
	Reverse: ACCTTCTCCTGCCGCAACTA

Quantitative PCR

RNA from confluent cultures was isolated using the QIAshredder and RNeasy Plus Mini Kits (Qiagen, Inc., Valencia, CA, USA) and cDNA was generated using the High Capacity cDNA Reverse Transcription Kit (Applied Biosystems, Foster City, CA, USA) according to the manufacturers' instructions. Quantitative (q)PCR was performed using a QuantStudio 7 Flex Real-Time PCR system and SYBR Green PCR Master Mix (both Thermo Fisher Scientific). Results were normalized to the housekeeping gene succinate dehydrogenase (SDHA). The primers (Integrated DNA Technologies, Coralville, IA, USA) used for the qPCR reactions are listed in the Table.

G-LISA RhoA Activation Assay

Confluent cultures of EV or CAβ3 cells were serum starved for ~16 hours prior to being left untreated or stimulated with 10% FBS for 15 or 30 minutes, respectively. Cells were then processed for analysis using the RhoA G-LISA activation assay kit (cat. #BK124; Cytoskeleton, Denver, CO, USA) according to the manufacturer's instructions. Briefly, cell lysates were incubated for 30 minutes at 4°C in microtiter wells that had been precoated with the Rho binding domain from a Rho effector protein, rhotekin, that specifically binds active RhoA. Wells were washed and incubated for 45 minutes at room temperature with a mouse anti-RhoA antibody. Wells were washed again and incubated with horseradish peroxidase (HRP)-conjugated goat anti-mouse IgG secondary antibody. The plates were then washed and the level of label in each well was detected using a HRP detection reagent provided by the manufacturer for 10 to 15 minutes at 37°C. The reaction was stopped with HRP stop buffer. Wells were read at 490 nm to determine the content of GTP-bound RhoA present in each well.

Investigative Ophthalmology & Visual Science

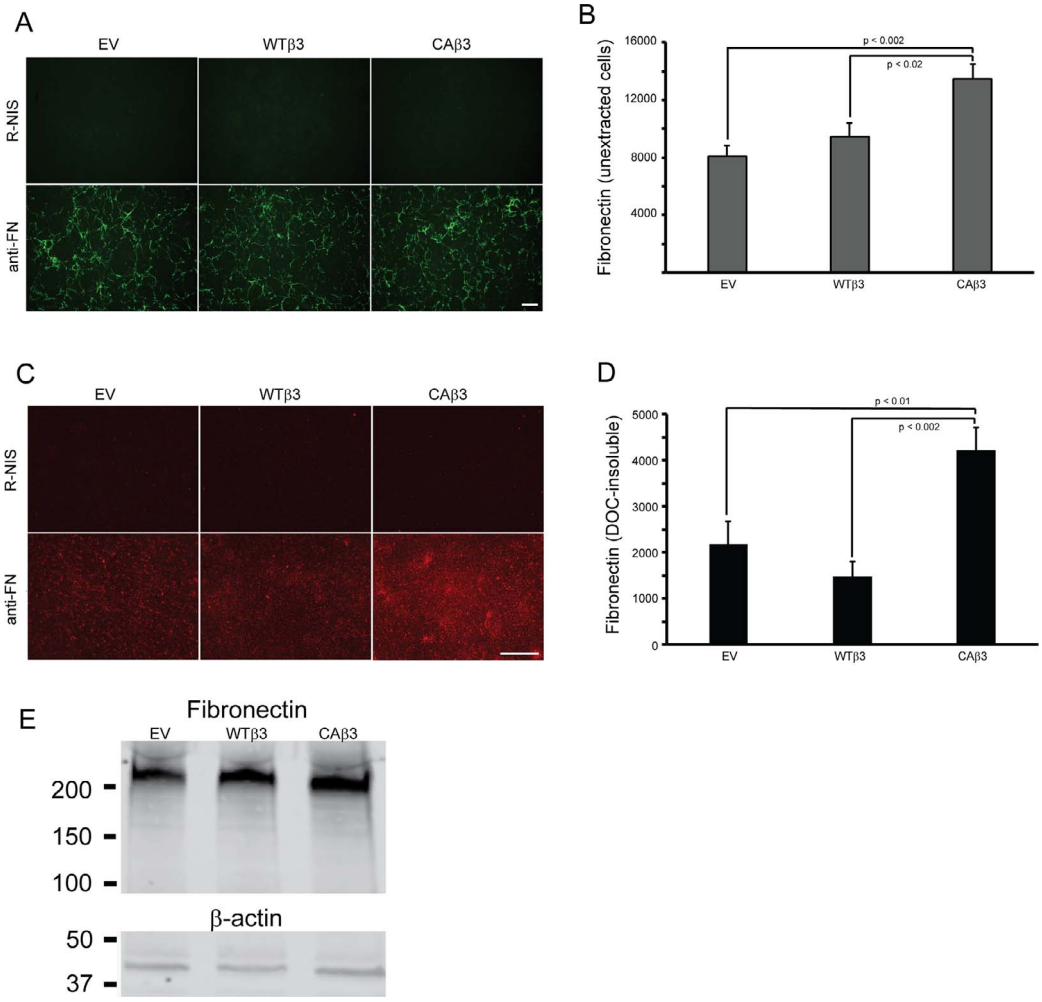

Figure 1. Constitutively active αvβ3 integrin signaling increases fibronectin matrix assembly in TM-1 cell lines. (**A**) Fibronectin fibrils in intact, confluent monolayers of TM-1 cells expressing an empty vector (EV) or overexpressing a wild-type (WTβ3) or constitutively active (CAβ3) β3 integrin subunit. Cells were labeled with either fibronectin polyclonal antiserum (anti-FN) or with rabbit nonimmune serum (R-NIS). *Scale bar*: 50 μm. (**B**) On-cell western (OCW) analysis of fibronectin levels in intact confluent monolayers of EV, WTβ3, and CAβ3 cells. Cells were cultured for 24 hours prior to fixation and processing for OCW analysis. CAβ3 cells exhibited significantly more fibronectin labeling than EV ($P < 0.002$) and WTβ3 ($P < 0.02$) cells. Data are pooled from six separate assays with triplicate determinations ($n = 18$) and represent the mean ± SE. (**C**) Immunofluorescence microscopy images of DOC-insoluble fibronectin fibrils from EV, WTβ3, and CAβ3 monolayers extracted with 1% DOC. Extracted cell layers were labeled with anti-FN serum or R-NIS. More intense labeling for DOC-insoluble fibronectin was observed from CAβ3 cultures compared to EV or WTβ3 cultures. *Scale bar*: 50 μm. (**D**) OCW analysis of levels of DOC-insoluble fibronectin fibrils from EV, WTβ3, and CAβ3 cultures. Cells were cultured for 24 hours prior to DOC extraction, fixation, and processing for OCW analysis. CAβ3 cells exhibited significantly more DOC-insoluble fibronectin labeling than EV ($P < 0.01$) and WTβ3 ($P < 0.002$) cells. Data are pooled from six separate assays with triplicate determinations ($n = 18$) and represent the mean ± SE. (**E**) Western blot analysis of fibronectin expression in whole cell lysates consisting of soluble and DOC-insoluble fibronectin from EV, WTβ3, and CAβ3 cells. Blots were labeled for either fibronectin (*top*) or β-actin (*bottom*). No differences in total fibronectin levels were observed between the three cell lines. This experiment was performed twice with similar results.

Statistical Analysis

Statistical analysis was performed using ANOVA. Where pairs of treatment groups were compared, ANOVA analysis was used in conjunction with Tukey's honestly significant difference test.

Results

Effect of Activation of β3 Integrin Signaling on Fibronectin Matrix Assembly in Immortalized TM Cells

To determine if αvβ3 integrin signaling influenced fibronectin fibrillogenesis, confluent monolayers of the EV cell line or cell lines overexpressing the WTβ3 or the CAβ3 integrin subunits were fixed and labeled for fibronectin (Fig. 1A). By immunofluorescence microscopy, no obvious differences in labeling patterns or intensity were observed in the two cell lines overexpressing the β3 integrin subunits compared to control EV cells. Quantification of the cell surface–labeled fibronectin using OCW analysis, however, showed a 1.7-fold increase ($P < 0.002$) in fibronectin in cells overexpressing a CAβ3 integrin subunit compared to EV cells (Fig. 1B). CAβ3 cultures also expressed a 1.4-fold increase ($P < 0.02$) in fibronectin compared to WTβ3 cultures, suggesting that the activation state of the integrin, rather than just overexpression, was affecting levels of fibronectin in the intact cell layer.

In order to differentiate between cell surface–bound soluble fibronectin and fibronectin assembled into an insoluble fibril, cell cultures were extracted with DOC. The DOC extraction

procedure removes soluble, cell surface–bound and intracellular fibronectin but not fibronectin assembled into insoluble fibrils. It is these insoluble fibrils that are the functional form of fibronectin that serve to support a variety of cell behaviors under both normal and pathological conditions in vivo.[19,55,56] As shown in Figure 1C, DOC-extracted monolayers immunolabeled for fibronectin showed a clear increase in fibronectin matrices formed by CAβ3 cultures compared to both EV and WTβ3 cultures (Fig. 1C). OCW analysis of the DOC-extracted monolayers (Fig. 1D) confirmed the immunofluorescence microscopy results and showed a ∼2-fold increase ($P < 0.01$) in DOC-insoluble fibrils in CAβ3 cultures compared to EV cultures. When compared to WTβ3 cultures, the CAβ3 cultures showed a ∼3-fold increase in DOC-insoluble fibrils ($P < 0.002$). Thus the increase in insoluble fibrils was not due to the mere overexpression of the β3 integrin subunit as a similar increase was not observed in the levels of insoluble fibrils expressed in the WTβ3 cultures compared to the EV cultures.

The increase in fibronectin fibrils was also not due to changes in the level of fibronectin expression, since Western blot analysis of whole cell lysates (Fig. 1E) did not show any consistent differences in fibronectin levels between the three cell lines. Interestingly, both WTβ3 and CAβ3 cells demonstrated a 1.5-fold increase in fibronectin mRNA levels ($P < 0.01$) compared to EV cells (Supplementary Fig. S1). However, there was no difference between fibronectin mRNA levels in WTβ3 and CAβ3 cells, indicating that differences in mRNA levels were not a factor in the observed differences in fibronectin fibril levels. In order to determine if differences in fibronectin isoform expression were a factor in this phenomenon, we also analyzed the mRNA levels of the EDA+ and EDB+ isoforms of fibronectin. As shown in Supplementary Figure S1, although the EDA+ fibronectin isoform appeared to be expressed at higher levels in both WTβ3 and CAβ3 cultures compared to EV cultures, the differences were not statistically significant. EDB+ fibronectin mRNA levels were comparable between the three cell lines.

We then wanted to verify that the WTβ3 and CAβ3 cells expressed similar levels of αvβ3 integrins on their cell surface given the differences in the levels of their assembled fibronectin matrices. FACS analysis using the mAb LM609 to αvβ3 integrin (Supplementary Fig. S2) confirmed our earlier study[40] and showed that EV cells express very low levels of αvβ3 integrin on the cell surface while WTβ3 and CAβ3 cells showed significantly higher levels of αvβ3 integrin. The cell surface levels of αvβ3 integrin in WTβ3 and CAβ3 cells, however, were comparable.

Effect of β3 Integrin Activation on Fibronectin Matrix Assembly in Normal HTM Cells

We next sought to confirm that activation of αvβ3 integrin signaling increased fibronectin matrix assembly in primary HTM cells. For this, HTM cells were cultured in the presence or absence of DEX, which we previously demonstrated led to the activation of αvβ3 integrin[38,41] and increased fibronectin matrix assembly,[12] with or without increasing concentrations of the cyclic RGD peptide CGT, which has been reported to activate αvβ3 signaling when used at high concentrations.[54] As shown in Figure 2A, HTM cells treated with vehicle together with 100 μM CGT demonstrated 2.7-fold more DOC-insoluble fibronectin matrix ($P < 0.005$) compared to cells treated with vehicle alone. Higher levels of DOC-insoluble matrix were also observed in the presence of 50 and 200 μM CGT; however, these levels were not significantly greater than with vehicle alone. In contrast, cells treated with DEX and all three CGT concentrations demonstrated significantly more DOC-insoluble fibronectin matrix ($P < 0.01$) compared to cells treated with DEX alone. Consistent with our earlier study,[12] DEX treatment by itself significantly increased DOC-insoluble fibronectin matrix compared to vehicle-treated cells ($P < 0.002$).

In a second set of experiments, HTM cells were transduced with Ad5 viral vectors expressing either WTβ3 or CAβ3 integrin-mCherry transgenes (Figs. 2B, 2C). An empty Ad5 viral vector (EV) was used as a control. Twelve days post transduction, OCW analysis showed that HTM cells transduced with Ad5-CAβ3 assembled 1.35-fold more DOC-insoluble fibronectin matrix compared to control cells transduced with Ad5-EV ($P < 0.003$). Ad5-CAβ3–transduced cells also assembled 1.2-fold more DOC-insoluble fibronectin matrix ($P < 0.03$) than cells transduced with Ad5-WTβ3. Together these data confirmed our findings using immortalized TM-1–derived cell lines that overexpressing an activated αvβ3 integrin enhances fibronectin fibril formation.

Effect of Overexpressing αvβ3 Integrins in TM Cells on α5β1 Integrin-Mediated Fibronectin Fibril Assembly

Because α5β1 integrin plays a significant role in fibronectin fibrillogenesis in most cells,[35,36] we also wanted to determine if α5β1 integrin levels were different in the three cell lines. FACS analysis using mAb P1D6 against the α5 integrin subunit (Fig. 3A) or mAb 12G10 against the β1 subunit (Fig. 3B) indicated that there were minor (≤1.2-fold) but statistically significant differences ($P < 0.001$) in α5 and β1 integrin subunit levels between the three cell lines. These differences did not, however, correlate with the observed differences in levels of fibronectin matrices formed by the three cell lines.

We next wanted to determine if the insoluble fibronectin fibrils formed in CAβ3 cultures involved the canonical α5β1 integrin–mediated processes commonly thought to regulate fibril formation (Fig. 4A).[12,31] In particular, we wanted to determine if antibodies to α5β1 integrin disrupted binding of soluble fibronectin to the cell surface and whether these fibrils were sensitive to disruption by the peptide FUD, which was previously found to disrupt fibronectin fibrillogenesis in HTM cultures.[12] For this, we treated EV, WTβ3, and CAβ3 cultures for 24 hours with either the β1 integrin function-blocking mAb 13, previously shown to block the early cell surface binding step in fibronectin matrix assembly,[35,36] or FUD. All three cell lines were then processed for OCW analysis and immunofluorescence microscopy.

In intact, unextracted cell layers (Fig. 4B), mAb 13 behaved as expected and treatment significantly decreased cell surface binding of fibronectin in all three cell lines. Decreases of 54%, 33%, and 32% (all $P < 0.01$) were seen in EV, WTβ3, and CAβ3 cell lines, respectively. Immunofluorescence microscopy verified the OCW analysis. As shown in Figure 4C, confluent monolayers of untreated EV, WTβ3, and CAβ3 cells form a well-developed fibronectin matrix. However, a 24-hour exposure to mAb 13 caused a marked reduction in fibronectin levels in all three cell lines, consistent with previous studies.[35,36] Thus, all three cell lines were using the α5β1 integrin to bind fibronectin and mediate the early cell surface steps in fibril formation. With respect to DOC-insoluble fibronectin fibrils (Fig. 4E), mAb 13 had little or no effect on the incorporation of the remaining cell surface–bound fibronectin into the insoluble ECM in all three cell lines.

Responses to FUD treatment in intact monolayers were similar. In both WTβ3 and CAβ3 cultures, FUD caused significant decreases of 39% and 42% in the level of fibronectin in intact cell layers (both $P < 0.01$), respectively, compared to untreated WTβ3 and CAβ3 cultures (Fig. 4B). In FUD-treated EV cultures the 25% reduction in fibrils was not quite

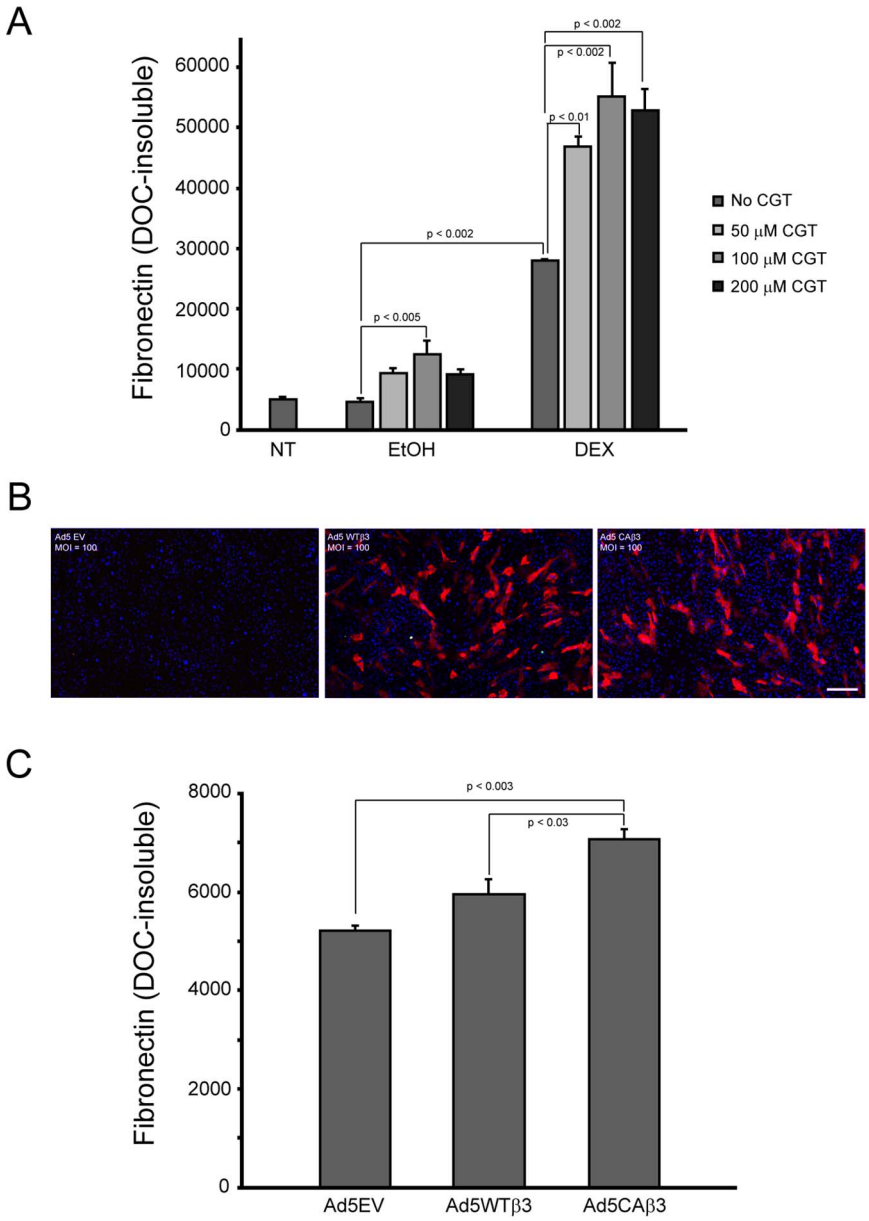

Figure 2. Activation of αvβ3 integrin signaling in normal HTM cells increases fibronectin matrix assembly. (**A**) Confluent monolayers of HTM cells were left untreated or treated for 12 days with vehicle (0.1% EtOH) or 500 nM DEX alone or in the presence of increasing concentrations of the CGT peptide. Cell layers were then extracted with 1% DOC and processed for OCW analysis. There was no difference in the levels of fibronectin fibrils between untreated cells and cells treated with EtOH alone. Cells treated with EtOH and 100 μM CGT showed significant increases in DOC-insoluble fibronectin levels compared to control cells treated with EtOH alone ($P < 0.005$). Although fibronectin levels were higher in cells treated with EtOH plus 50 or 200 μM CGT, the increases were not statistically significant. DEX treatment alone also significantly increased DOC-insoluble fibronectin levels relative to cells treated with EtOH alone ($P < 0.002$). In the presence of all three CGT concentrations, DOC-insoluble fibronectin fibril levels were significantly increased further in DEX-treated cells relative to DEX treatment alone (50 μM CGT, $P < 0.01$; 100 and 200 μM CGT, $P < 0.002$). The data reported are from one experiment that was performed twice with similar results. (**B**) Immunofluorescence microscopy images of HTM cells transduced with Ad5-EV or Ad5-WTβ3-mCherry or Ad5-CAβ3-mCherry viral vectors. Subconfluent cells were transduced at an MOI of 100 and processed for immunofluorescence 12 days post transduction. *Scale bar*: 500 μm. (**C**) OCW analysis of 1% DOC-extracted HTM cell monolayers transduced with Ad5 vectors described in (**B**). Twelve days post transduction, Ad5-CAβ3–transduced cells significantly increased DOC-insoluble fibronectin fibrils relative to both Ad5-EV–transduced cells ($P < 0.003$) and Ad5-WTβ3–transduced cells ($P < 0.03$). The data reported are from one experiment that was performed twice with similar results.

statistically significant ($P = 0.08$) compared to untreated EV cultures. These results were confirmed by immunofluorescence microscopy (Fig. 4D), which showed that treatment with FUD for 24 hours clearly reduced fibril formation in confluent monolayers of EV, WTβ3, and CAβ3. These results are consistent with our earlier study.[12] That earlier study also confirmed that the effects of the FUD were specific, as a mutated version of the peptide had little or no effect on fibronectin fibril assembly by TM-1 cells.

FUD also appeared to have an inhibitory effect on insoluble fibronectin fibril formation in EV and WTβ3 cultures (34% and 23%, respectively), but neither of these decreases was

Investigative Ophthalmology & Visual Science

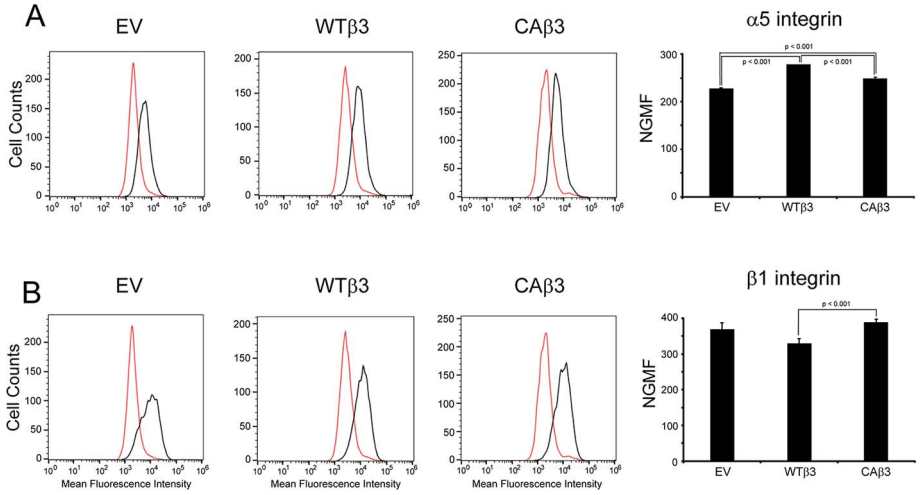

Figure 3. α5 and β1 integrin levels in EV, WTβ3, and CAβ3 cell lines. FACS analysis was performed on EV, WTβ3, and CAβ3 cells using (**A**) mAb PD16 (*black*) against the α5 integrin subunit or (**B**) mAb 12G10 (*black*) against the β1 integrin subunit. For both profiles, mouse IgG (*red*) was used as a control. Representative FACS profiles for each cell line are shown for each antibody. Each profile is from one analysis using duplicate determinations. The normalized geometric mean fluorescence (NGMF) for each antibody was determined by pooling data from two analyses, both using duplicate determinations ($n = 4$). The three cell lines demonstrated minor, statistically significant differences in α5 integrin levels (all $P < 0.001$) that did not correlate with differences in fibronectin fibril assembly. A minor, statistically significant difference ($P < 0.04$) between β1 integrin levels in WTβ3 and CAβ3 cells was also found; however, no difference was found in β1 integrin levels when EV and CAβ3 cells were compared. NGMF results represent the mean ± SE.

statistically significant. In contrast, FUD significantly decreased fibronectin incorporation into the insoluble ECM in CAβ3 cell cultures, with the peptide causing a 45% decrease in fibronectin levels ($P < 0.01$). Thus, the assembly of fibronectin fibrils in these cells appears to follow the canonical α5β1 integrin–mediated process in which binding of fibronectin to the cell surface is dependent upon α5β1 integrins while later steps in fibril formation, such as those involving fibronectin–fibronectin interactions, are sensitive to FUD inhibition.

In order to verify that the loss of fibronectin fibrils in response to FUD was not due to any cytotoxic effects of the peptide, MTT assays were performed on all three cell lines in the presence or absence of FUD (Supplementary Fig. S3). Interestingly, there was some mild, statistically significant cytotoxicity in response to 500 nM FUD in both the EV and WTβ3 cultures. The degree of cytotoxicity did not change, however, in the presence of 2 μM FUD, suggesting that the low level of cytotoxicity in response to the peptide was maximal. In contrast, the CAβ3 cells were resistant to this cytotoxicity, which is similar to what was observed when primary HTM cells were treated with FUD.[12]

Localization of α5β1 and αvβ3 Integrins in Fibrillar Adhesions and Focal Adhesions in TM Cells Overexpressing αvβ3 Integrins

We sought to further confirm that this canonical α5β1 integrin–mediated mechanism was present in TM-1 cells and was being used in CAβ3 cultures. To that end, we double-labeled subconfluent cultures of EV, WTβ3, and CAβ3 cells for nascent fibronectin fibrils and activated α5β1 integrins using the SNAKA51 antibody (Fig. 5). SNAKA51 is an antibody that specifically recognizes activated α5β1 integrins present within the main sites of fibronectin matrix assembly called fibrillar adhesions (Fig. 4A).[57–59] As shown in Figure 5, all three cell lines exhibited extensive colocalization of activated α5β1 integrins (Figs. 5D, 5G, 5J) and fibronectin (Figs. 5E, 5H, 5K) in fibrillar adhesions.

We next sought to determine if activated αvβ3 integrins also localized to fibrillar adhesions in CAβ3 cultures where fibronectin fibrillogenesis was occurring and whether this could explain the enhanced fibronectin fibril assembly observed in these cells. For this we utilized the mAb CRC54,[60] which we previously used to detect activated αvβ3 integrins in TM cells.[41] Consistent with our earlier studies,[40] little or no activated αvβ3 integrin was detected in EV cells. Neither focal adhesions (sites of cell attachment) nor fibrillar adhesions in EV cells contained activated αvβ3 integrin, although there were abundant fibronectin fibrils present (Figs. 6A–C). We also did not see any activated αvβ3 integrins in fibrillar adhesions in either WTβ3 or CAβ3 cells. However, activated αvβ3 integrins were found in focal adhesion complexes in both WTβ3 and CAβ3 cultures (Figs. 6D, 6G). Not surprisingly, these αvβ3 integrin-positive focal adhesion complexes were more prominent in CAβ3 cells compared to WTβ3 cells. In both cell lines, however, few if any of the αvβ3-integrin–positive focal adhesion complexes colocalized with fibronectin fibrils (Figs. 6F, 6I). Thus, activated αvβ3 integrins were not involved in the sites of fibronectin fibril assembly. CRC54-positive structures were confirmed to be focal adhesions by double-labeling cultures of all three cell lines with phalloidin, to visualize actin stress fibers and either mAb LM609 (Supplementary Fig. S4) or mAb CRC54 (Supplementary Fig. S5).

Effect of Inhibiting ROCK Activity on the Incorporation of Fibronectin Fibrils Into the DOC-Insoluble Matrix

We next sought to determine whether or not RhoA was involved in the enhanced incorporation of fibronectin into the DOC-insoluble fibrils exhibited by CAβ3 cells, since it is well established that Rho GTPase signaling plays a role in regulating fibronectin fibrillogenesis in TM cells and other cell types.[34,61–64] We first compared the level of RhoA activity in EV cells and CAβ3 cells in response to serum stimulation (Fig. 7). Since EV and WTβ3 cells behaved the same in earlier

Investigative Ophthalmology & Visual Science

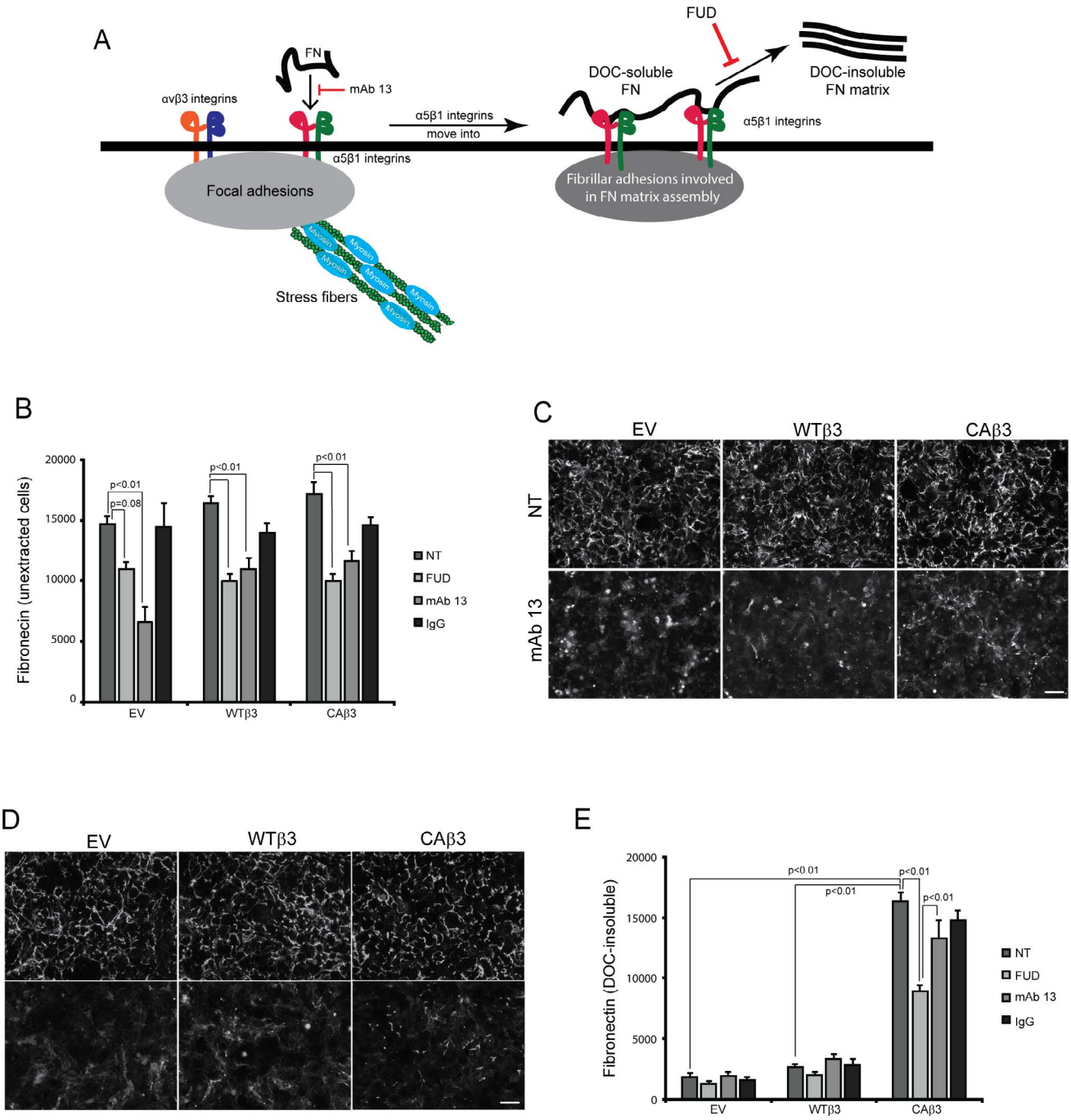

Figure 4. Both mAb 13 and FUD inhibit fibronectin fibril formation. (**A**) Schematic showing the canonical α5β1 integrin–mediated pathway involved in fibronectin fibrillogenesis.[58] As previously reported,[46] both α5β1 and αvβ3 integrins can colocalize to focal adhesions in TM cells. During the initial stages of fibril formation, soluble fibronectin dimers bound to α5β1 integrins are unfolded within focal adhesions together with αvβ3 integrins. The fibronectin–α5β1 integrin complex, but not αvβ3 integrin, is then translocated to regions of fibril formation called fibrillar adhesions.[58] While in fibrillar adhesions, fibronectin–fibronectin binding interactions promote the assembly of DOC-insoluble fibrils. Both the β1 integrin function-blocking mAb 13 and FUD inhibit this process as indicated in the schematic. (**B**) OCW analysis of unextracted confluent monolayers of EV, WTβ3, and CAβ3 cells. Cells were left untreated (NT) or treated for 24 hours with 500 nM FUD, 10 μg/mL mAb 13, or control IgG. Monoclonal Ab 13 significantly reduced fibronectin fibril formation in all three cell lines ($P < 0.01$) while FUD significantly reduced fibril formation in the WTβ3 and CAβ3 cells, respectively ($P < 0.01$). The ~25% reduction in response to FUD seen in the EV cultures was not statistically significant ($P = 0.08$). Data are pooled from two separate assays with triplicate determinations ($n = 6$) and represent the mean ± SE. (**C**) Immunofluorescence images of intact, unextracted monolayers of EV, WTβ3, and CAβ3 cells that were left untreated or treated with 10 μg/mL mAb 13 for 24 hours prior to labeling with rabbit fibronectin antiserum. Monoclonal Ab 13 disrupted fibronectin fibril formation in all three cell lines. The labeling is a combination of both soluble and insoluble fibronectin fibrils. *Scale bar*: 50 μm. (**D**) Immunofluorescence images of intact, unextracted confluent monolayers of EV, WTβ3, and CAβ3 cells that were left untreated or treated with 500 nM FUD for 24 hours prior to labeling with rabbit fibronectin antiserum. FUD disrupted fibronectin fibril formation in all three cell lines. The labeling is a combination of both soluble and insoluble fibronectin fibrils. *Scale bar*: 50 μm. (**E**) OCW analysis of DOC-extracted monolayers of EV, WTβ3, and CAβ3 cells. Cells were treated as in (**B**) prior to DOC extraction; mAb 13 did not have an effect on DOC-insoluble fibronectin levels in any of the three cell lines. FUD only statistically significantly decreased DOC-insoluble fibronectin levels in the CAβ3 cell cultures relative to both untreated cells and cells treated with mAb 13 (both $P < 0.01$). The minor decreases in the insoluble fibronectin matrices seen in both EV and WTβ3 cells were not statistically significant. Comparing untreated groups, CAβ3 cells exhibited significantly more DOC-insoluble fibronectin matrix than either EV or WTβ3 cells, respectively ($P < 0.01$). Data are pooled from two separate assays with triplicate determinations ($n = 6$) and represent the mean ± SE.

Investigative Ophthalmology & Visual Science

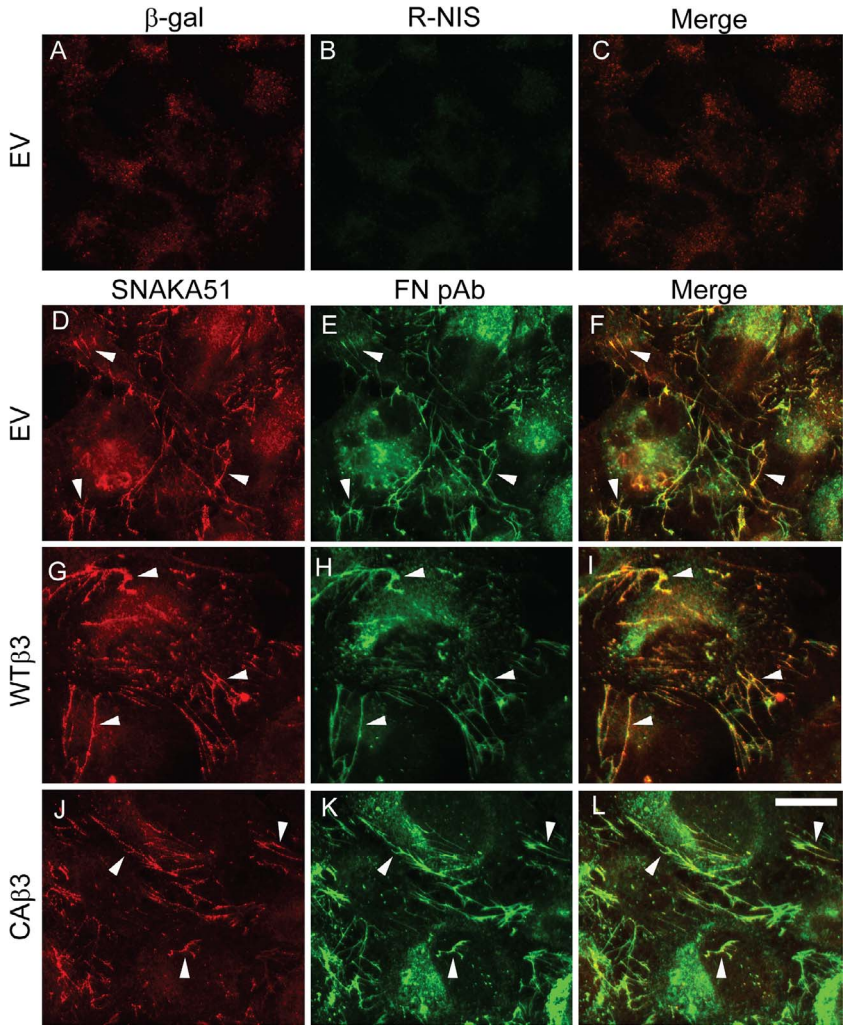

Figure 5. Constitutively active αvβ3 signaling does not alter α5β1 integrin localization within fibrillar adhesions. Subconfluent EV, WTβ3, or CAβ3 cells were plated onto glass coverslips for 24 hours prior to fixation. Cells were double-labeled with mAb SNAKA51 against the active α5β1 integrin (**D**, **G**, **J**) and rabbit anti-fibronectin antiserum (FN) (**E**, **H**, **K**). As a control, EV cells (**A**–**C**) were double-labeled with mAb GAL-13 against β-galactosidase (**A**) and R-NIS (**B**). Extensive colocalization (*arrowheads*) of α5β1 integrin and fibronectin within fibrillar adhesions was observed in all three cell lines (**F**, **I**, **L**). WTβ3 and CAβ3 cells (not shown) were also double-labeled with mAb GAL-13 and R-NIS with identical results as observed with EV cells. This labeling was performed three times with identical results. *Scale bar*: 50 μm.

experiments, we used only EV cells in this set of experiments. EV cells exhibited a weak, transient, and statistically insignificant ($P = 0.28$) 23% increase in RhoA activity in response to serum that peaked at 15 minutes post stimulation. CAβ3 cells also exhibited a weak increase in RhoA activity 15 minutes post serum stimulation; however, by 30 minutes, RhoA activity had significantly increased 37% over control levels ($P < 0.02$) and 30% over the levels seen at 15 minutes ($P < 0.045$).

Given that CAβ3 cells appeared to exhibit a higher level of RhoA activity compared to EV cells, we then examined whether or not the enhanced fibronectin fibrillogenesis in CAβ3 cells was mediated by RhoA signaling. For this study, we treated confluent monolayers of EV, WTβ3, and CAβ3 cells with or without the Y27632 inhibitor, which targets the downstream effector of RhoA called ROCK. Phase microscopy of inhibitor-treated cells (Supplementary Fig. S6) showed that all three cell lines responded to Y27632 and exhibited retraction and/or cell rounding compared to untreated cells. The enhanced level of fibronectin in the insoluble matrix of CAβ3 cultures, however, was unaffected by the presence of the ROCK inhibitor (Fig. 8A). In fact, Y27632 had no effect on the levels of fibronectin insoluble matrices in all three cell lines. In addition to there being no significant loss of DOC-insoluble fibronectin fibrils, immunofluorescence microscopy analysis of the three cell lines treated with or without Y27632 showed that the only obvious change in the inhibitor-treated cells was an increase in punctate labeling for fibronectin (Fig. 8B). Z-stack and three-dimensional reconstruction analysis of images acquired from control and inhibitor-treated EV, WTβ3, and CAβ3 cultures showed that the punctate labeling was predominantly intracellular (Supplementary Fig. S7)

Effect of Overexpressing αvβ3 Integrins on the Incorporation of Structurally Different Fibronectin Fibrils Into the Insoluble ECM of TM Cells

We then considered the possibility that constitutively active αvβ3 integrin signaling changed the structure of the fibronectin in fibrils assembled by CAβ3 cells. Thus, we first used the mAb L8, which recognizes a conformation-sensitive epitope

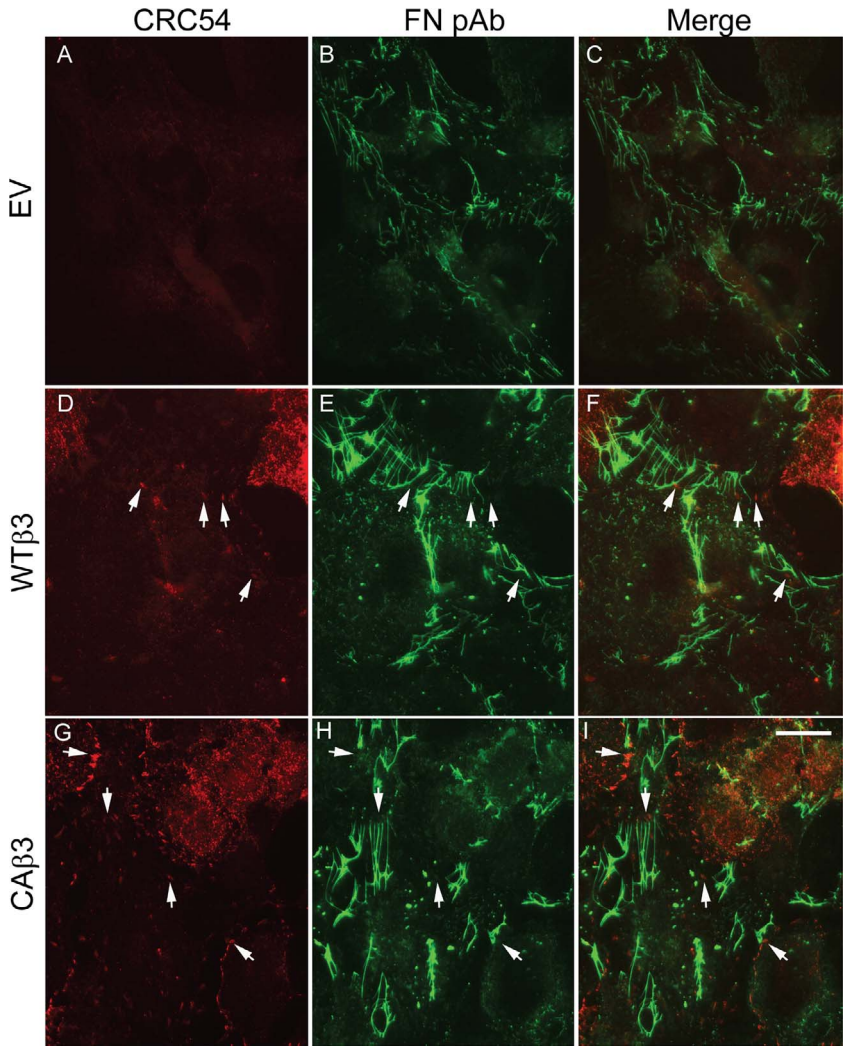

Figure 6. Constitutively active αvβ3 integrin localizes in focal adhesions but fails to localize in fibrillar adhesions. Cells were plated as in Figure 5. Cells were double-labeled with mAb CRC54 that detects activated αvβ3 integrin (**A**, **D**, **G**) and rabbit anti-fibronectin antiserum (FN) (**B**, **E**, **H**). Activated αvβ3 integrin was not detectable in EV cells (**A**). *Arrows* indicate sites of αvβ3 integrin localization that fail to colocalize with fibronectin fibrils as shown when the red and green channels are merged (**C**, **F**, **I**). Control cells were double-labeled with mAb GAL-13 and R-NIS (not shown) with identical results as observed in Figure 5. This labeling was performed twice with identical results. *Scale bar*: 50 μm.

that is exposed within fibronectin fibrils that have had their quaternary structure unfolded and their tertiary and/or secondary structure stretched in response to cell-derived mechanical forces (Fig. 9A).[34,65] Analysis of intact monolayers by immunofluorescence microscopy (Fig. 9B) indicated no obvious differences in L8 labeling between the three cell lines. OCW analysis of intact monolayers (Fig. 9C), however, found that WTβ3 cultures demonstrated L8 labeling that was 1.3- to 1.45-fold lower than in EV ($P < 0.02$) or CAβ3 ($P < 0.005$) cultures, respectively. In contrast, CAβ3 cultures had significantly higher levels of L8 labeling in DOC-insoluble fibronectin fibrils than the other two cell lines (Fig. 9D). The difference in L8 labeling was 5.7-fold ($P < 0.005$) comparing CAβ3 and EV cultures while the difference between CAβ3 and WTβ3 cultures was 2.6-fold ($P < 0.02$). This indicates that fibronectin in the fibrils assembled by CAβ3 cells was more unfolded or stretched compared to the fibronectin in fibrils assembled by the other cell lines.

We then used mAbs IST-9 and BC-1 that detect the alternatively spliced EDA+ and EDB+ domains in fibronectin (Fig. 10A), respectively, to determine if fibrils assembled by CAβ3 cells contained different fibronectin isoforms. As shown in Figure 10B, immunofluorescence microscopy of intact monolayers labeled with mAb IST-9 suggested that CAβ3 cell layers contained slightly more EDA+ fibronectin than the other two cell lines. OCW analysis of intact monolayers (Fig. 10C) confirmed this, although the increase in labeling was not statistically significant. However, there was at least 4-fold more DOC-insoluble EDA+ fibronectin (Fig. 10D) in CAβ3 cultures compared to the other two cell lines (both $P < 0.002$). Together these data suggest that although the three cell lines may be expressing the same total levels of EDA+ fibronectin, CAβ3 cell are assembling more EDA+ fibronectin into DOC-insoluble fibrils.

Using mAb BC-1 to detect EDB+ fibronectin in fibrils, both immunofluorescence microscopy (Fig. 10B) and OCW analysis (Fig. 10C) showed that intact monolayers of EV cells labeled significantly stronger for this isoform than WTβ3 cells ($P < 0.002$) and CAβ3 cells ($P < 0.02$). Labeling for EDB+ fibronectin in fibrils in intact cultures of EV cells was 2.5- and 1.5-fold greater than that seen in WTβ3 and CAβ3 cultures, respectively. In contrast, when we examined the levels of

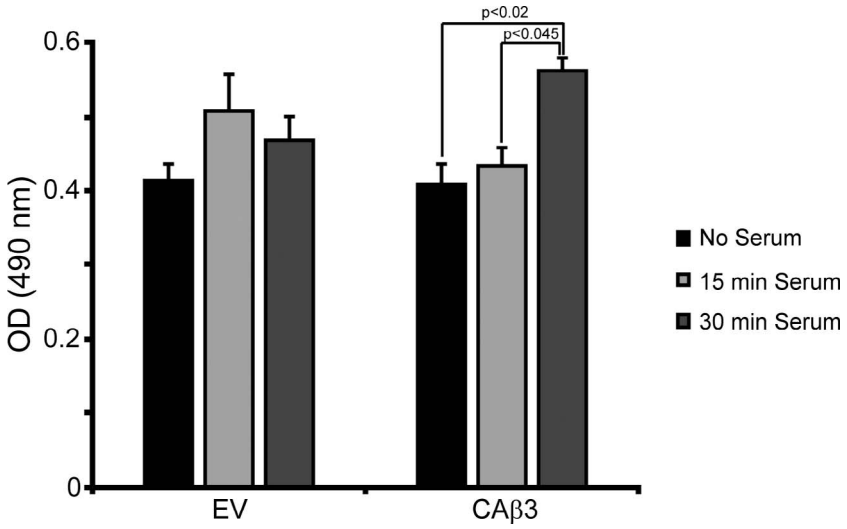

Figure 7. CAβ3 cells demonstrate elevated RhoA activity in response to serum. EV and CAβ3 cells were serum starved for ~16 hours prior to simulation with 10% FBS for 15 or 30 minutes prior to G-LISA analysis. EV cells failed to demonstrate statistically significant RhoA activation under these conditions. CAβ3 cells responded to serum after 30 minutes with a significant increase in RhoA activity ($P < 0.02$) over untreated cells or cells treated for 15 minutes with serum ($P < 0.045$). Results are pooled from three separate assays with triplicate determinations ($n = 9$) and represent the mean ± SE.

EDB+ fibronectin fibrils in cultures extracted with DOC (Fig. 10D), we found that CAβ3 cells incorporated at least 17-fold more DOC-insoluble EDB+ fibronectin fibrils compared to both EV and WTβ3 cultures (both $P < 0.03$). Thus, both the composition (EDA+/EDB+ isoforms) and stretched conformation of fibronectin in fibrils made by CAβ3 cells appear to be different compared to the fibrils assembled by EV and WTβ3 cells.

Discussion

In this study we have shown that activation of αvβ3 integrins in TM cells enhances fibronectin fibrillogenesis. This is consistent with our earlier studies that found that HTM cells treated with glucocorticoids expressed higher levels of activated αvβ3 integrins[38,40,41] and these cells assembled higher levels of DOC-insoluble fibronectin matrices.[12] These fibrils are formed using an alternative ROCK-independent pathway and appear to have different structural properties and composition. Such differences are likely to alter the signaling properties of the ECM and behavior of TM cells.[66] Theoretically these differences could contribute to the development of pathological changes observed in glaucoma, especially SIG, where the αvβ3 integrin is likely to be activated.[38,67]

This is not the first time an integrin other than α5β1, the main integrin responsible for mediating fibronectin fibril assembly,[35,36] has been found to be involved in fibronectin fibril formation. There are a limited number of other integrin heterodimers that can promote fibronectin fibrillogenesis, including αvβ3 integrins,[68–70] which in some instances appear to play a more significant role in matrix assembly than α5β1 integrins.[71] These earlier studies are consistent with the results presented here demonstrating a pronounced enhancement in fibronectin fibrillogenesis in TM cells overexpressing constitutively active αvβ3 integrins.

The increase in fibril formation was not due to a disruption in the canonical α5β1 integrin–mediated fibronectin fibril assembly mechanism that appeared to be functioning in TM cells, including those overexpressing a constitutively active β3 integrin. These studies show that mAb 13, which blocks binding of fibronectin to α5β1 integrins in the early stages of fibril formation, was able to block binding of fibronectin in CAβ3 cultures, suggesting that this early integrin-mediated step was still involved. In addition, fibrillar adhesions, which are the sites where fibronectin fibrils are assembled, only contained α5β1 integrins, further suggesting that an α5β1 integrin step was involved. In contrast, αvβ3 integrins were not found in fibrillar adhesions, implying that αvβ3 integrins were not involved in the initial binding of fibronectin during fibril formation. This suggests that the enhanced deposition of fibronectin fibrils in CAβ3 cells may be due to αvβ3 integrin playing a role in the later stages of fibril formation when the transition of cell surface–soluble fibronectin into insoluble fibrils occurs[72] and/or it is altering the signaling pathways that govern fibronectin fibril formation.

How αvβ3 integrin signaling is affecting fibril formation is still unclear. The increased assembly of these fibronectin fibrils could be due to the enhanced RhoA activity of the CAβ3 cells in response to serum (see Fig. 7). Early studies demonstrated that fibronectin fibrillogenesis is a RhoA-dependent process,[34,61] and RhoA signaling has also been suggested to play a role in regulating fibronectin matrix formation in TM cell cultures.[62] RhoA activity has also been reported to be upregulated when the β3 integrin subunit is overexpressed.[73] The changes in RhoA activity would influence the contractile state and traction force generated by a cell through sites of focal adhesions, which in turn can significantly impact a cell's ability to assemble a fibronectin matrix.[34,59,74] The implication here is that traction and contractile forces on fibronectin promote unfolding and stretching of the fibronectin dimer, which in turn initiates a cascade of intermolecular interactions between multiple fibronectin dimers that propagate the formation of a DOC-insoluble fibril. Such an enhanced unfolding and stretching of fibronectin's conformation was seen in CAβ3 cells when we labeled the matrices with the L8 antibody that recognizes a conformation-sensitive epitope.

Interestingly, when we tried to use the ROCK inhibitor Y27632 to correlate the increased incorporation of fibronectin into the DOC-insoluble matrix with RhoA signaling, we failed to see a decrease in fibronectin fibril formation. Earlier studies

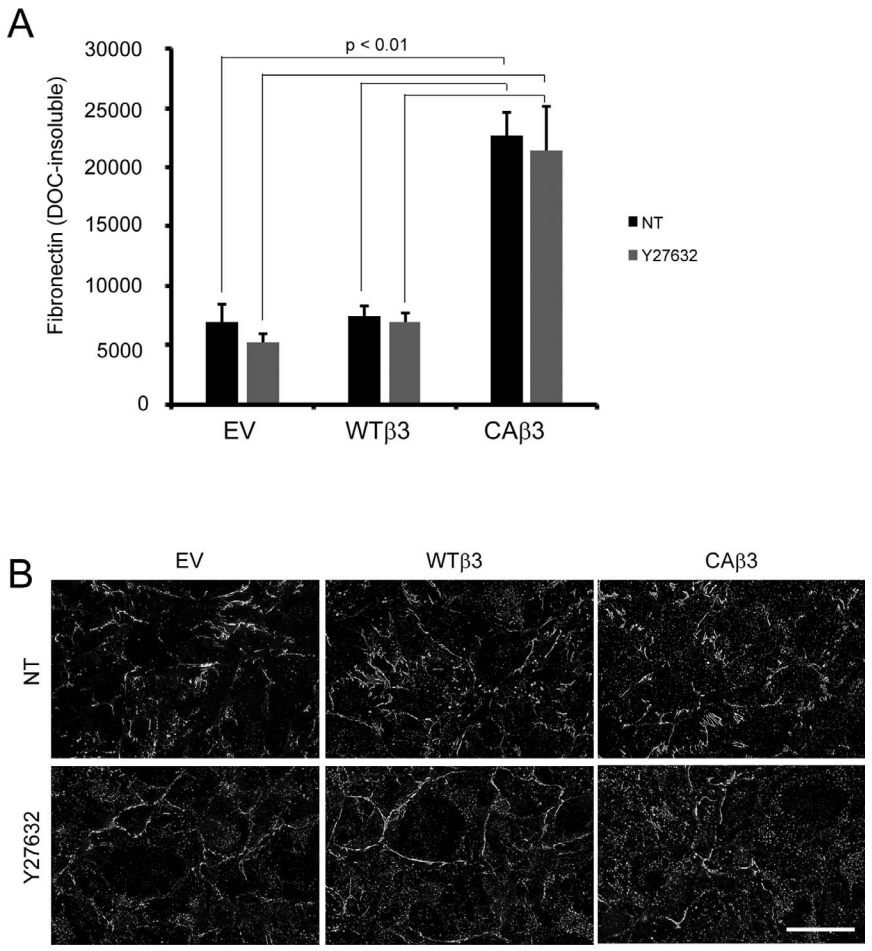

Figure 8. DOC-insoluble fibronectin matrix assembly is independent of ROCK activity. (**A**) OCW analysis of EV, WTβ3, and CAβ3 cells treated with or without 5 μM Y27632 ROCK inhibitor for 24 hours prior to extraction with 1% DOC and subsequent fixation. CAβ3 cells exhibited significantly enhanced matrix assembly relative to both EV and WTβ3 cells in the absence and presence of the ROCK inhibitor (all $P < 0.01$). Data are pooled from two separate assays with triplicate determinations ($n = 6$) and represent the mean ± SE. (**B**) Compressed Z-stack images of intact, confluent monolayers of EV, WTβ3, and CAβ3 cells treated as in (**A**) prior to DOC extraction and labeled with rabbit anti-fibronectin antiserum. Although the fibronectin fibrils are relatively unchanged in the inhibitor-treated cells, there was an apparent increase in intracellular punctate fibronectin labeling (see Supplementary Fig. S7) in the inhibitor-treated cells. *Scale bar*: 50 μm.

have suggested that other pathways, independent of RhoA/ROCK, can play a role in fibronectin fibrillogenesis. Studies by Hill et al.[17] showed that when living rat eyes were treated with TGFβ1 there was an increase in fibronectin that was only modestly decreased by inhibiting RhoA activity using siRNA. A similar result has also been reported in endothelial cells that appear to be capable of assembling a fibronectin matrix in the absence of a classical RhoA-dependent pathway.[63] Additional studies in *Xenopus* embryos[75] and human foreskin fibroblasts[58] also suggested that RhoA/ROCK-independent pathways could play a significant role in promoting fibronectin fibrillogenesis.

Together these observations support our data that a RhoA/ROCK signaling pathway does not appear to play a significant role in the enhanced fibronectin matrix deposition by CAβ3 cells. Instead, there appears to be a ROCK-independent pathway that is mediating enhanced fibril formation in these cells. Studies by Shiller et al.[76] have recently proposed that an alternative RhoA-mediated pathway can control contractility and hence may be involved in fibril formation. In this alternative pathway (Fig. 11), the RhoA/ROCK pathway is mediated to a large extent by α5β1 integrin signaling while signaling via αv-class integrins such as αvβ3 mediates RhoA signaling via the guanine nucleotide exchange factor (GEF) GEF-H1 and the formin mDia. Other studies support this idea. Zamir et al.[58] found that fibrillar adhesion formation (hence fibrillogenesis) occurred via a RhoA/ROCK-independent mechanism while another study found that inhibiting mDia blocked fibrillar adhesion formation and impaired fibronectin remodeling.[77] Other alternative pathways have also been proposed. Fernandez-Sauze et al.[63] have proposed an alternative Rho-independent mechanism involving ILK and Rac1 that could be responsible for the phosphorylation of myosin light chain and the generation of the contractile forces needed for matrix assembly. Thus, it is possible that the CAβ3 cells are utilizing one or both of these pathways to control the contractile forces that enhance fibronectin matrix assembly.

These studies also showed that the composition and stretched state of fibronectin in fibrils appeared to be altered in CAβ3 cells. Our studies indicate that the DOC-insoluble fibrils in cultures of CAβ3 cells contain substantially more EDA+ and/or EDB+ fibronectin than those assembled by EV or WTβ3 cells. This was despite the fact that intact EV and CAβ3 monolayers demonstrated comparable levels of EDA+ fibronectin and EV monolayers exhibited significantly more EDB+ fibronectin labeling than either WTβ3 or CAβ3 cultures. Yet

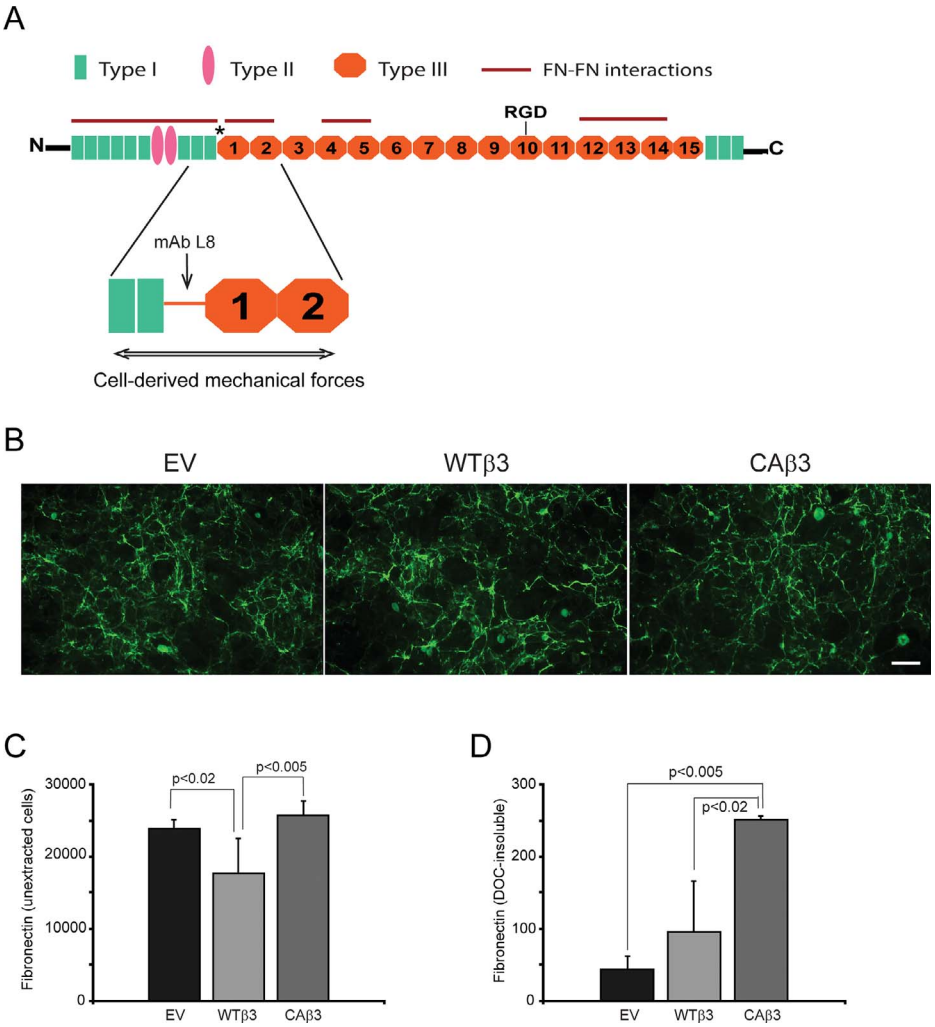

Figure 9. Constitutively active αvβ3 integrin increases deposition of L8+, stretched fibronectin in fibrils within the DOC-insoluble matrix. (**A**) A fibronectin monomer consists of repeating modules called type I (*green*), type II (*pink*), and type III repeats (*orange*). The L8 mAb recognizes an epitope in the first type III repeat that becomes accessible to the antibody when the protein is unfolded and/or stretched in response to tension caused by cell-derived mechanical forces.[34] The sites that mediate fibronectin–fibronectin intermolecular interactions are indicated by the *red lines*. RGD, the primary integrin-binding site within the 10th type III repeat. (**B**) Intact, confluent monolayers of EV, WTβ3, and CAβ3 cells were immunolabeled with mAb L8. Negative control cells were labeled with mAb GAL-13 against β-galactosidase and showed no significant labeling (not shown). No clear differences in L8 labeling were observed between the three cell lines. This experiment was performed twice with identical results. *Scale bar*: 50 μm. (**C**) OCW analysis of intact, confluent monolayers of EV, WTβ3, and CAβ3 cells plated for 24 hours. WTβ3 cells demonstrated less L8 labeling than both EV cells ($P < 0.02$) and CAβ3 cells ($P < 0.005$). There was no difference between EV and CAβ3 cells. Results represent the mean ± SE and consist of data pooled from two assays using quadruplicate and triplicate determinations, respectively ($n = 7$). (**D**) OCW analysis of DOC-insoluble fibronectin fibrils in monolayers after being extracted with 1% DOC. CAβ3 cells demonstrated significantly higher levels of DOC-insoluble L8+ fibronectin fibrils than both EV cells ($P < 0.005$) and WTβ3 cells ($P < 0.02$). Results represent the mean ± SE and consist of data pooled from two assays using triplicate determinations ($n = 6$).

very little EDA+ and/or EDB+ fibronectin could be detected in the insoluble matrix of EV cells. This suggests that activation of αvβ3 integrin is involved in promoting the assembly of fibronectin fibrils that include one or both of these domains.

Interestingly, cultured HTM cells treated with either glucocorticoids, which can cause αvβ3 integrin activity to be upregulated, or TGFβ2 can both upregulate the EDA+ and EDB+ fibronectin isoforms.[11,12] In addition, EDA+ fibronectin has been reported to be elevated in glaucomatous TM tissues.[11] This suggests, especially in SIG, that αvβ3 integrin activity may be involved in ECM deposition in these circumstances.

In addition to this change in fibril composition, our studies indicate that there is a higher percentage of L8 labeling in the DOC-insoluble fibrils found in CAβ3 cultures. Since the L8 antibody detects an epitope that is exposed when fibronectin is stretched or unfolded in response to cell-derived mechanical forces,[34,65,78,79] this suggests that fibronectin in fibrils in CAβ3 cultures may be under more tension or mechanical forces.

This enhanced unfolding and/or stretching of fibronectin fibrils is associated with more rigid fibrils in aging matrices and would be expected to have different biochemical properties that would affect cell behavior.[78] The observation that EDB+ fibronectin is more prevalent in fibrils assembled by CAβ3 cells further substantiates this idea that fibrils assembled when αvβ3 integrin is activated have different biological properties. Together these studies show that activation of αvβ3 integrins,

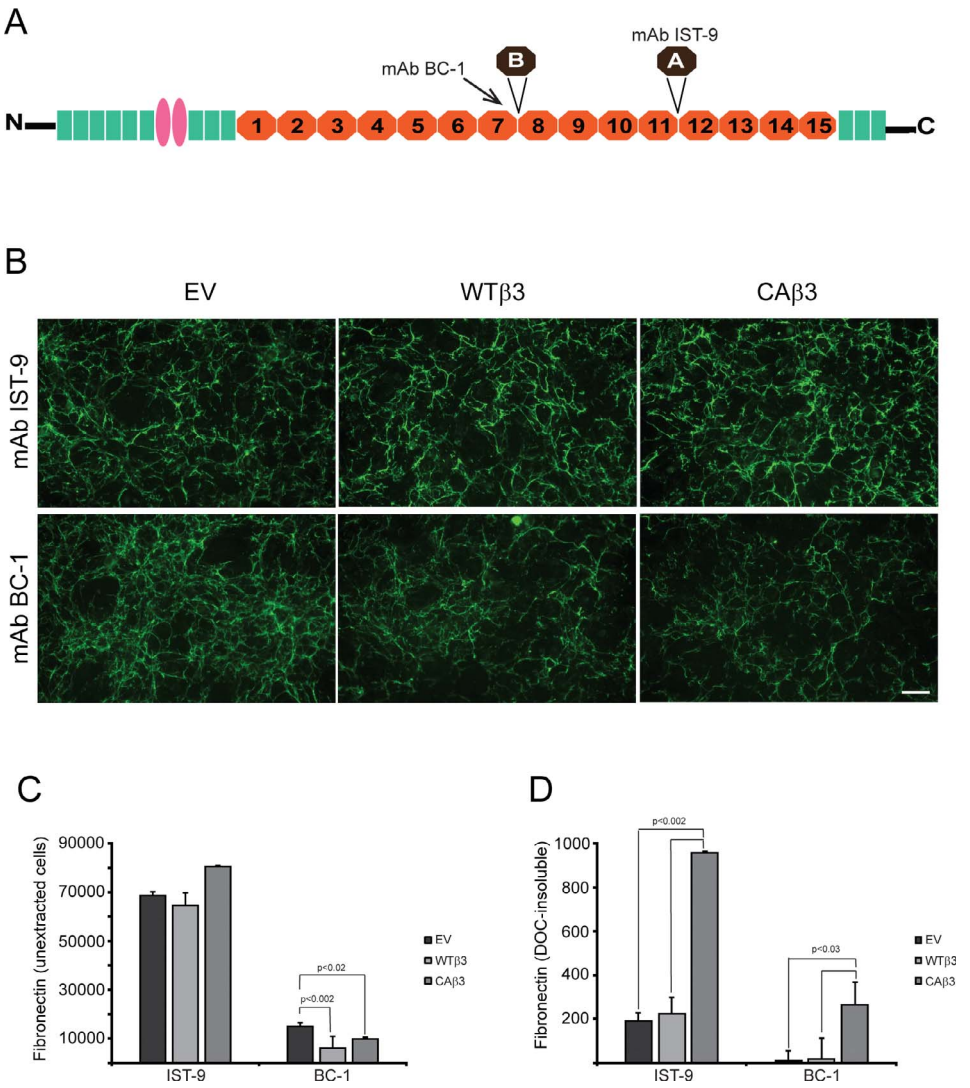

Figure 10. Constitutively active αvβ3 integrin increases deposition of specific fibronectin isoforms into the DOC-insoluble matrix. (**A**) Fibronectin schematic showing the locations of the EDA and EDB alternatively spliced domains. The mAb BC-1 recognizes a conformation-specific epitope formed in the seventh type III repeat when the EDB domain is present.[85] The IST-9 mAb detects a sequence found within the EDA domain. (**B**) Intact, confluent monolayers of EV, WTβ3, and CAβ3 cells were immunolabeled with mAbs IST-9 and BC-1, respectively. No clear differences in labeling intensity were observed between the three cell lines for mAb IST-9. EV cells, however, demonstrated more intense labeling with mAb BC-1 than both WTβ3 and CAβ3 cells. Negative control cells were labeled with mAb GAL-13 against β-galactosidase and showed no significant labeling (not shown). This experiment was performed twice with identical results. *Scale bar*: 50 μm. (**C**) OCW analysis of intact, unextracted monolayers of EV, WTβ3, and CAβ3 cells plated for 24 hours. No significant difference was found between any of the three cell lines with respect to EDA+ fibronectin. Both WTβ3 cells ($P < 0.002$) and CAβ3 cells ($P < 0.02$) demonstrated less EDB+ fibronectin in intact monolayers relative to EV cells. Results represent the mean ± SE and consist of data pooled from two assays using quadruplicate and triplicate determinations, respectively ($n = 7$). (**D**) OCW analysis of DOC-insoluble fibronectin fibrils in EV, WTβ3, and CAβ3 cultures. CAβ3 cells demonstrated significantly higher levels of DOC-insoluble EDA+ fibronectin fibrils than EV and WTβ3 cells ($P < 0.002$). CAβ3 cells demonstrated significantly higher levels of DOC-insoluble EDB+ fibronectin fibrils than EV and WTβ3 cells ($P < 0.03$). Results represent the mean ± SE and consist of data pooled from two assays using triplicate determinations ($n = 6$).

especially by glucocorticoids, may result in the assembly of a fibronectin matrix with biological properties that differs from a matrix assembled under conditions where αvβ3 integrin is either expressed at very low levels such as in EV cells or not active such as in WTβ3 cells. Whether these changes could contribute to the enhanced rigidity of the ECM associated with glaucoma is unknown.

In summary, in addition to the β3 integrin–induced alteration in fibronectin fibrillogenesis shown here, earlier work from our lab also found that β3 integrin signaling played a role in altering the TM cytoskeleton to form CLANs[41,46,47] and served as a negative regulator of TM phagocytosis.[40,80] Collectively, alterations in these biological processes are associated with the pathogenesis of certain forms of glaucoma such as POAG and SIG.[67,81–83] This suggests that dysregulation of β3 integrin signaling may play a significant role in the pathogenesis of these glaucomas and possibly other forms of the disease. Future studies using the tamoxifen-inducible *Cre*$^{+/-}$ β3 *integrin*$^{flox/flox}$ mouse model we recently developed to knock down expression of αvβ3 integrin in the trabecular meshwork[84] should help determine the role of this integrin in POAG.

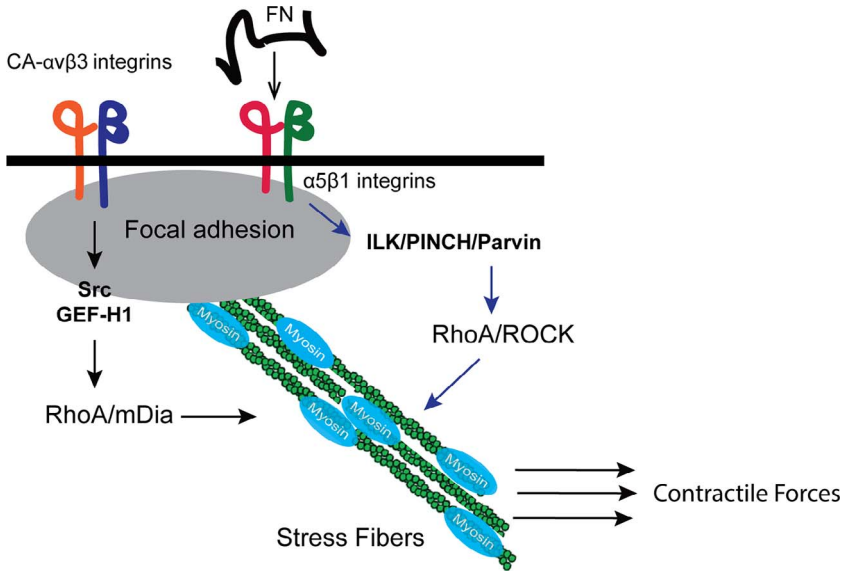

Figure 11. Proposed mechanism for how αvβ3 integrin signaling could be mediating fibronectin matrix assembly in TM cells. Recent studies by Schiller et al.[76] suggest that there are alternative ways in which stress fibers can be assembled by integrin signaling. Signaling from α5β1 integrins can activate a RhoA/ROCK-dependent signaling pathway that results in myosin phosphorylation. In contrast, αvβ3 integrin signaling can use a separate ROCK-independent pathway that utilizes RhoA/mDia, which promotes enhanced F-actin polymerization that is required for the formation of stress fibers. In addition, these actin filaments are necessary for the formation of fibrillar adhesions that are the sites of fibronectin fibrillogenesis.[77] Together these two processes lead to stronger contractile forces that could ultimately lead to the enhanced fibronectin matrix assembly demonstrated by CAβ3 cells.

Acknowledgments

Supported by National Eye Institute Grants EY017006 and EY026009 (D.M.P.) and a Core Grant to the Department of Ophthalmology and Visual Sciences (P30 EY016665).

Disclosure: **M.S. Filla**, None; **J.A. Faralli**, None; **H. Desikan**, None; **J.L. Peotter**, None; **A.C. Wannow**, None; **D.M. Peters**, None

References

1. Quigley HA. Glaucoma. *Lancet*. 2011;377:1367–1377.
2. Braunger BM, Fuchshofer R, Tamm ER. The aqueous humor outflow pathways in glaucoma: a unifying concept of disease mechanisms and causative treatment. *Eur J Pharmaceut Biopharmaceut*. 2015;95:173–181.
3. Pattabiraman PP, Toris CB. The exit strategy: pharmacological modulation of extracellular matrix production and deposition for better aqueous humar drainage. *Eur J Pharmacol*. 2016; 787:32–42.
4. Stamer WD, Acott T. Current understanding of conventional outflow dysfunction in glaucoma. *Curr Opin Ophthalmol*. 2012;23:301–314.
5. Keller KE, Aga M, Bradley JM, Kelley MJ, Acott TS. Extracellular matrix turnover and outflow resistance. *Exp Eye Res*. 2009;88:676–682.
6. Wang C, Li L, Zhicheng L. Experimental research on the relationship between the stiffness and the expressions of fibronectin proteins and adaptor proteins of rat trabecular meshwork cells. *BMC Ophthalmol*. 2017;17:1–9.
7. Johnson D, Gottanka J, Flugel C, Hoffmann F, Futa R, Lütjen-Drecoll E. Ultrastructural changes in the trabecular meshwork of human eyes treated with corticosteroids. *Arch Ophthalmol*. 1997;115:375–383.
8. Lütjen-Drecoll E, Futa R, Rohen JW. Ultrahistochemical studies on tangential sections of the trabecular meshwork in normal and glaucomatous eyes. *Invest Ophthalmol Vis Sci*. 1981;21: 563–573.
9. Babizhayev MA, Brodskaya MW. Fibronectin detection in drainage outflow system of human eyes in ageing and progression of open-angle glaucoma. *Mech Ageing Dev*. 1989;47:145–157.
10. Fuchshofer R, Tamm ER. The role of TGF-β in the pathogenesis of primary open-angle glaucoma. *Cell Tissue Res*. 2011;347:279–290.
11. Medina-Ortiz WE, Belmares R, Neubauer S, Wordinger RJ, Clark AF. Cellular fibronectin expression in human trabecular meshwork and induction by transforming growth factor-β2. *Invest Ophthalmol Vis Sci*. 2013;54:6779–6788.
12. Filla MS, Dimeo KD, Tong T, Peters DM. Disruption of fibronectin matrix affects type IV collagen, fibrillin and laminin deposition into extracellular matrix of human trabecular meshwork (HTM) cells. *Exp Eye Res*. 2017;165: 7–19.
13. Steely HT, Browder SL, Julian MB, Miggans ST, Wilson KL, Clark AF. The effects of dexamethasone on fibronectin expression in cultured human trabecular meshwork cells. *Invest Ophthalmol Vis Sci*. 1992;33:2242–2250.
14. Zhou L, Li Y, Yue BY. Glucocorticord effects on extracellular matrix proteins and integrins in bovine trabecular meshwork cells in relation to glaucoma. *Int J Mol Med*. 1998;1:339–346.
15. Kasetti RB, Maddineni P, Patel PD, Searby C, Sheffield VC, Zode GS. Transforming growth factor β2 (TGFβ2) signaling plays a key role in glucocorticoid-induced ocular hypertension. *J Biol Chem*. 2018;293:9854–9868.
16. Hill LJ, Mead B, Blanch RJ, et al. Decorin reduces intraocular pressure and retinal ganglion cell loss in rodents through fibrolysis of the scarred trabecular meshwork. *Invest Ophthalmol Vis Sci*. 2015;56:3743–3757.
17. Hill LJ, Mead B, Thomas CN, et al. TGF-β-induced IOP elevations are mediated by RhoA in the early but not the late fibrotic phase of open angle glaucoma. *Mol Vis*. 2018;24: 712–726.
18. Acott TS, Kelley MJ. Extracellular matrix in the trabecular meshwork. *Exp Eye Res*. 2008;86:543–561.

19. Faralli JA, Schwinn MK, Gonzalez JM, Filla MS, Peters DM. Functional properties of fibronectin in the trabecular meshwork. *Exp Eye Res*. 2009;88:689–693.
20. Faralli JA, Dimeo KD, Trane RM, Peters D. Absence of a secondary glucocorticoid response in C57BL/6J mice treated with topical dexamethasone. *PLoS One*. 2018;13:e0192665.
21. Hynes RO. *Fibronectins*. New York: Springer-Verlag; 1990.
22. Sottile J, Hocking DC. Fibronectin polymerization regulates the composition and stability of extracellular matrix fibrils and cell-matrix adhesions. *Mol Biol Cell*. 2002;13:3546–3559.
23. Sabatier L, Chen D, Fagotto-Kaufmann C, et al. Fibrillin assembly requires fibronectin. *Mol Biol Cell*. 2009;20:846–858.
24. Velling T, Risteli J, Wennerberg K, Mosher DF, Johansson S. Polymerization of type I and III collagens is dependent on fibronectin and enhanced by integrins $\alpha_{11}\beta_1$ and $\alpha_2\beta_1$. *J Biol Chem*. 2002;277:37377–37381.
25. Li S, Van Den Diepstraten C, D'Souza SJ, Chan BMC, Pickering JG. Vascular smooth muscle cells orchestrate the assembly of type I collagen via α2β1 integrin, RhoA, and fibronectin polymerization. *Am J Pathol*. 2003;163:1045–1056.
26. Dallas SL, Sivakumar P, Jones CJP, et al. Fibronectin regulates latent transforming growth factor β (TGFβ) by controlling matrix assembly of latent TGFb-binding protein-1. *J Biol Chem*. 2005;280:18871–18880.
27. Fogelgren B, Polgár N, Szauter KM, et al. Cellular fibronectin binds to lysyl oxidase with high affinity and is critical for its proteolytic activation. *J Biol Chem*. 2005;280:24690–24697.
28. Wu M, Zhu X-Y, Ye J. Associations of polymorphisms of *LOXL1* gene with primary open-angle glaucoma: a meta-analysis based on 5,293 subjects. *Mol Vis*. 2015;21:165–172.
29. Serini G, Bochaton-Piallat ML, Ropraz P, et al. The fibronectin domain ED-A is crucial for myofibroblastic phenotype induction by transforming growth factor-β1. *J Cell Biol*. 1998;142:873–881.
30. Wolanska KI, Morgan MR. Fibronectin remodelling: cell mediated regulation of the microenvironment. *Biochem Soc Trans*. 2015;43:122–128.
31. Gagen D, Faralli JA, Filla MS, Peters DM. The role of integrins in the trabecular meshwork. *J Ocul Pharmcol Ther*. 2014;30:110–120.
32. Schwarzbauer JE, DeSimone DW. Fibronectin, their fibrillogenesis, and in vivo functions. *Cold Spring Harb Perspect Biol*. 2011;3:1–19.
33. Singh P, Carraher C, Schwarzbauer JE. Assembly of fibronectin extracellular matrix. *Annu Rev Cell Dev Biol*. 2010;26:397–419.
34. Zhong C, Chrzanowska-Wodnicka M, Brown J, Shaub A, Belkin AM, Burridge K. Rho-mediated contractility exposes a cryptic site in fibronectin and induces fibronectin matrix assembly. *J Cell Biol*. 1998;141:539–551.
35. Akiyama SK, Yamada SS, Chen WT, Yamada KM. Analysis of fibronectin receptor function with monoclonal antibodies: roles on cell adhesion, migration, matrix assembly, and cytoskeletal organization. *J Cell Biol*. 1989;109:863–875.
36. Fogerty FJ, Akiyama SK, Yamada KM, Mosher DF. Inhibition of binding of fibronectin to matrix assembly sites by anti-integrin (α5β1) antibodies. *J Cell Biol*. 1990;111:699–708.
37. Dickerson JE Jr, Steely HT Jr, English-Wright SL, Clark AF. The effect of dexamethasone on integrin and laminin expression in cultured human trabecular meshwork cells. *Exp Eye Res*. 1998;66:731–738.
38. Faralli JA, Gagen D, Filla MS, Crotti TN, Peters DM. Dexamethasone increases αvβ3 integrin expression and affinity through a calcineurin/NFAT pathway. *Biochim Biophys Acta*. 2013;1833:3306–3313.
39. Clark R, Nosie A, Walker T, et al. Comparative genomic and proteomic analysis of cytoskeletal changes in dexamethasone-treated trabecular meshwork cells. *Mol Cell Proteomics*. 2013;12:194–206.
40. Gagen D, Filla MS, Clark R, Liton P, Peters DM. Activated αvβ3 integrin regulates αvβ5 integrin–mediated phagocytosis in trabecular meshwork cells. *Invest Ophthalmol Vis Sci*. 2013;54:5000–5011.
41. Filla MS, Schwinn MK, Nosie AK, Clark RW, Peters DM. Dexamethasone-associated cross-linked actin network (CLAN) formation in human trabecular meshwork (HTM) cells involves β3 integrin signaling. *Invest Ophthalmol Vis Sci*. 2011;52:2952–2959.
42. Kagami S, Takashi K, Yasutomoa K, et al. Transforming growth factor-β (TGF-β) stimulates the expression of β1 integrins and adhesion by rat mesangial cells. *Exp Cell Res*. 1996;229:1–6.
43. Pechkovsky DV, Scaffidi AK, Hackett TL, et al. Transforming growth factor β1 induces αvβ3 integrin expression in human lung fibroblasts via a β3 integrin-, c-Src-, and p38 MAPK-dependent pathway. *J Biol Chem*. 2008;283:12898–12908.
44. Mori S, Kodaira M, Ito A, et al. Enhanced expression of integrin αvβ3 induced by TGF-β is required for the enhancing effect of fibroblast growth factor 1 (FGF1) in TGF-β-induced epithelial-mesenchymal transition (EMT) in mammary epithelial cells. *PLoS One*. 2015;10:1–18.
45. Tsukamoto T, Kajiwara K, Nada S, Okada M. Src mediates TGF-β-induced intraocular pressure elevation in glaucoma. *J Cell Physiol*. 2018;34:1730–1744.
46. Filla MS, Woods A, Kaufman PL, Peters DM. β1 and β3 integrins cooperate to induce syndecan-4 containing cross-linked actin networks (CLANs) in human trabecular meshwork (HTM) cells. *Invest Ophthalmol Vis Sci*. 2006;47:1956–1967.
47. Filla MS, Schwinn MK, Sheibani N, Kaufman PL, Peters DM. Regulation of cross-linked actin network (CLAN) formation in human trabecular meshwork (HTM) cells by convergence of distinct β1 and β3 integrin pathways. *Invest Ophthalmol Vis Sci*. 2009;50:5723–5731.
48. Dzamba BJ, Wu H, Jaenisch R, Peters DM. Fibronectin binding site in type I collagen regulates fibronectin fibril formation. *J Cell Biol*. 1993;121:1165–1172.
49. Chernousov MA, Faerman AI, Frid MG, Printseva OY, Koteliansky VE. A monoclonal antibody to fibronectin which inhibits extracellular matrix assembly. *FEBS Lett*. 1987;217:124–128.
50. Kashiwagi H, Tomiyama Y, Tadokoro S, et al. A mutation in the extracellular cysteine-rich repeat region of the β3 subunit activates integrins αIIbβ3 and αvβ3. *Blood*. 1999;93:2559–2568.
51. Filla MS, David G, Weinreb RN, Kaufman PL, Peters DP. Distribution of syndecans 1-4 within the anterior segment of the human eye: expression of a variant syndecan-3 and matrix associated syndecan-2. *Exp Eye Res*. 2004;79:61–74.
52. Polansky JR. HTM cell culture model for steroid effects on intraocular pressure: overview. In: Lutjen-Drecoll E, ed. *Basic Aspects of Glaucoma Research III*. Stuttgart: Schattauer Verlag; 1993:307–318.
53. Polansky JR, Alvarado JA. Cellular mechanisms influencing the aqueous humor outflow pathway. In: Albert D, Jakobiec FA, eds. *Principles and Practice of Ophthalmology: Basic Sciences*. Philadelphia: W.B. Saunders; 1994:226–251.
54. Alghisi GC, Ponsonnet L, Rüegg C. The integrin antagonist cilengitide activates αvβ3, disrupts VE-cadherin localization at cell junctions and enhances permeability in endothelial cells. *PLoS One*. 2009;4:e4449.
55. Chen LB, Murray A, Segal RA, Bushnell A, Walsh ML. Studies on intercellular LETS glycoprotein matrices. *Cell*. 1978;14:377–391.

Investigative Ophthalmology & Visual Science

56. Christopher RA, Kowalczyk AP, McKeown-Longo PJ. Localization of fibronectin matrix assembly sites on fibroblasts and endothelial cells. *J Cell Sci*. 1997;110:569–581.
57. Clark K, Pankov R, Travis MA, et al. A specific α5β1-integrin conformation promotes directional integrin translocation and fibronectin matrix formation. *J Cell Sci*. 2005;118:291–300.
58. Zamir E, Katz M, Posen Y, et al. Dynamics and segregation of cell–matrix adhesions in cultured fibroblasts. *Nat Cell Biol*. 2000;2:191–196.
59. Pankov R, Cukierman E, Katz B-Z, et al. Integrin dynamics and matrix assembly: tensin-dependent translocation of α5β1 integrins promotes early fibronectin fibrillogenesis. *J Cell Biol*. 2000;148:1075–1090.
60. Mazurov AV, Khaspekova SG, Byzova TV, et al. Stimulation of platelet glycoprotein IIb-IIIa ($\alpha_{IIb}\beta_3$-integrin) functional activity by a monoclonal antibody to the N-terminal region of glycoprotein IIIa. *FEBS Lett*. 1996;391:84–88.
61. Zhang Q, Magnusson MK, Mosher DF. Lysophosphatidic acid and microtubule-destabilizing agents stimulate fibronectin matrix assembly through Rho-dependent actin stress fiber formation and cell contraction. *Mol Biol Cell*. 1997;8:1415–1425.
62. Pattabiraman PP, Rao PV. Mechanistic basis of Rho GTPase-induced extracellular matrix synthesis in trabecular meshwork cells. *Am J Physiol Cell Physiol*. 2010;298:C749–C763.
63. Fernandez-Sauze S, Grall D, Cseh B, Van Obberghen-Schilling E. Regulation of fibronectin matrix assembly and capillary morphogenesis in endothelial cells by Rho family GTPases. *Exp Cell Res*. 2009;315:2092–2104.
64. Torr EE, Ngam CR, Bernau K, Tomasini-Johansson B, Acton B, Sandbo N. Myofibroblasts exhibit enhanced fibronectin assembly that is intrinsic to their contractile phenotype. *J Biol Chem*. 2015;290:6951–6961.
65. Smith ML, Gourdon D, Little WC, et al. Force-induced unfolding of fibronectin in the extracellular matrix of living cells. *PLoS Biol*. 2007;5:2243–2254.
66. Turner CJ, Badu-Nkansah K, Hynes RO. Endothelium-derived fibronectin regulates neonatal vascular morphogenesis in an autocrine fashion. *Angiogenesis*. 2017;20:519–531.
67. Filla MS, Faralli JA, Peotter JL, Peters DM. The role of integrins in glaucoma. *Exp Eye Res*. 2017;158:124–136.
68. Wennerberg K, Lohikangas L, Gullberg D, Pfaff M, Johansson S, Fässler R. β1 Integrin-dependent and -independent polymerization of fibronectin. *J Cell Biol*. 1996;132:227–238.
69. Sechler JL, Cuminsky AM, Gazzola DM, Scwarzbauer JE. A novel RGD-independent fibronectin assembly pathway initiated by alpha4beta1 integrin binding to the alternatively spliced V region. *J Cell Sci*. 2000;113:1491–1498.
70. Yang JT, Hynes RO. Fibronectin receptor functions in embryonic cells deficient in α5β1 integrin can be replaced by av integrins. *Mol Biol Cell*. 1996;7:1737–1748.
71. Attieh Y, Clark GA, Crass C, et al. Cancer-associated fibroblasts lead tumor invasion through integrin-β3–dependent fibronectin assembly. *J Cell Biol*. 2017;216:3509–3520.
72. McKeown-Longo PJ, Mosher DF. Binding of plasma fibronectin to cell layers of human skin fibroblasts. *J Cell Biol*. 1983;98:22–28.
73. Miao H, Li S, Hu YL, et al. Differential regulation of Rho GTPases by beta1 and beta3 integrins: the role of an extracellular domain of integrin in intracellular signaling. *J Cell Sci*. 2002;115:2199–2206.
74. Gee EPS, Yüksel D, Stultz CM, Ingber DE. SLLISWD sequence in the 10FNIII domain initiates fibronectin fibrillogenesis. *J Biol Chem*. 2013;288:21329–21340.
75. Dzamba BJ, Jakab KR, Marsden M, Schwartz MA, DeSimon DW. Cadherin adhesion, tissue tension, and noncanonical Wnt signaling regulate fibronectin matrix organization. *Dev Cell*. 2009;163:421–432.
76. Schiller HB, Hermann MR, Polleux J, et al. β1- and αv-class integrins cooperate to regulate myosin II during rigidity sensing of fibronectin-based microenvironments. *Nat Cell Biol*. 2013;15:625–636.
77. Oakes PW, Beckham Y, Stricker J, Gardel ML. Tension is required but not sufficient for focal adhesion maturation without a stress fiber template. *J Cell Biol*. 2012;196:363–374.
78. Antia M, Baneyx G, Kubow KE, Vogel V. Fibronectin in aging extracellular matrix fibrils is progressively unfolded by cells and elicits an enhanced rigidity response. *Faraday Discuss*. 2008;139:229–249.
79. Baneyx G, Baugh L, Vogel V. Coexisting conformations of fibronectin in cell culture imaged using fluorescence resonance energy transfer. *Proc Natl Acad Sci U S A*. 2001;98:14464–14468.
80. Faralli JA, Desikan H, Peotter J, et al. Genomic/proteomic analyses of dexamethasone (DEX)-treated human trabecular meshwork (TM) cells reveal a role for GULP1 and ABR in phagocytosis. *Mol Vis*. 2019;25:237–254.
81. Clark AF, Wordinger RJ. The role of steroids in outflow resistance. *Exp Eye Res*. 2009;88:752–759.
82. Clark AF. The cell and molecular biology of glaucoma: biomechanical factors in glaucoma. *Invest Ophthalmol Vis Sci*. 2012;53:2473–2475.
83. Liton PB. The autophagic lysosomal system in outflow pathway physiology and pathophysiology. *Exp Eye Res*. 2016;144:29–37.
84. Faralli JA, Filla MS, Peters DM. Effect of αvβ3 integrin expression and activity on intraocular pressure regulation of IOP by αvβ3 integrin. *Invest Ophthalmol Vis Sci*. 2019;60:1776–1788.
85. Carnemolla B, Baiza E, Siri A, et al. A tumor-associated fibronectin isoform generated by alternative splicing of messenger RNA precursors. *J Cell Biol*. 1989;108:1139–1148.

Investigative Ophthalmology & Visual Science